

On the Habitability of Our Universe

Abraham Loeb

Astronomy department, Harvard University, 60 Garden Street, Cambridge, MA 02138, USA

E-mail: aloeb@cfa.harvard.edu

Abstract. Is life most likely to emerge at the present cosmic time near a star like the Sun? We consider the habitability of the Universe throughout cosmic history, and conservatively restrict our attention to the context of “life as we know it” and the standard cosmological model, Λ CDM. The habitable cosmic epoch started shortly after the first stars formed, about 30 Myr after the Big Bang, and will end about 10 Tyr from now, when all stars will die. We review the formation history of habitable planets and find that unless habitability around low mass stars is suppressed, life is most likely to exist near $\sim 0.1M_{\odot}$ stars ten trillion years from now. Spectroscopic searches for biosignatures in the atmospheres of transiting Earth-mass planets around low mass stars will determine whether present-day life is indeed premature or typical from a cosmic perspective.

Contents

1	Introduction	2
2	The Habitable Epoch of the Early Universe	2
2.1	Section Background	2
2.2	First Planets	3
2.3	Section Summary and Implications	4
3	CEMP stars: possible hosts to carbon planets in the early universe	5
3.1	Section Background	5
3.2	Star-forming environment of CEMP stars	6
3.3	Orbital Radii of Potential Carbon Planets	8
3.4	Mass-Radius Relationship for Carbon Planets	12
3.5	Transit Properties	14
3.6	Section Summary and Implications	18
4	Water Formation During the Epoch of First Metal Enrichment	20
4.1	Section Background	20
4.2	Model Ingredients	21
4.3	Chemical Model	22
4.4	Time scales	22
4.5	Results	24
4.6	$x_{\text{H}_2\text{O}}$ as a function of T and I_{UV}/n_4	24
4.7	Variations in Z' and $\zeta_{-16}/I_{\text{UV}}$	25
4.8	Section Summary and Implications	25
5	An Observational Test for the Anthropic Origin of the Cosmological Constant	26
5.1	Section Background	26
5.2	Prior Probability Distribution of Vacuum Densities	27
5.3	Extragalactic Planet Searches	28
5.4	Observations of Dwarf Galaxies at High-redshifts	29
5.5	Section Summary and Implications	29
6	The Relative Likelihood of Life as a Function of Cosmic Time	31
6.1	Section Background	31
6.2	Formalism	31
6.2.1	Master Equation	31
6.2.2	Stellar Mass Range	32
6.2.3	Time Range	32
6.2.4	Initial Mass Function	33
6.2.5	Stellar Lifetime	33
6.2.6	Star Formation Rate	34
6.2.7	Probability of Life on a Habitable Planet	34
6.3	Results	35

1 Introduction

The known forms of terrestrial life involve carbon-based chemistry in liquid water [1, 2]. In the cosmological context, life could not have started earlier than 10 Myr after the Big Bang ($z \gtrsim 140$) since the entire Universe was bathed in a thermal radiation background above the boiling temperature of liquid water. Later on, however, the Universe cooled to a *habitable epoch* at a comfortable temperature of 273-373 K between 10-17 Myr after the Big Bang [3], as discussed in §2.

The phase diagram of water allows it to be liquid only under external pressure in an atmosphere which can be confined gravitationally on the surface of a planet. To keep the atmosphere bound against evaporation requires strong surface gravity of a rocky planet with a mass comparable to or above that of the Earth [4].

Life requires stars for two reasons. Stars are needed to produce the heavy elements (carbon, oxygen and so on, up to iron) out of which rocky planets and the molecules of life are made. Stars also provide a heat source for powering the chemistry of life on the surface of their planets. Each star is surrounded by a habitable zone where the surface temperature of a planet allows liquid water to exist. The approximate distance of the habitable zone, r_{HZ} , is obtained by equating the heating rate per unit area from the stellar luminosity, L , to the cooling rate per unit area at a surface temperature of $T_{\text{HZ}} \sim 300$ K, namely $(L/4\pi r_{\text{HZ}}^2) \sim \sigma T_{\text{HZ}}^4$, where σ is the Stefan-Boltzman constant [2].

According to the standard model of cosmology, the first stars in the observable Universe formed ~ 30 Myr after the Big Bang at a redshift, $z \sim 70$ [3, 5–7]. Within a few Myr, the first supernovae dispersed heavy elements into the surrounding gas, enriching the second generation stars with heavy elements. Remnants from the second generation of stars are found in the halo of the Milky Way galaxy, and may have planetary systems in the habitable zone around them [8], as discussed in §3. The related planets are likely made of carbon, and water could have been delivered to their surface by icy comets, in a similar manner to the solar system. The formation of water is expected to consume most of the oxygen in the metal poor interstellar medium of the first galaxies [9], as discussed in §4. Therefore, even if the cosmological constant was bigger than its measured value by up to a factor of $\sim 10^3$ so that galaxy formation was suppressed at redshifts $z \lesssim 10$, life could have still emerged in our Universe due to the earliest generation of galaxies [10], as discussed in §5.

In the following sections of this chapter we discuss the habitability of the Universe as a function of cosmic time. We conclude in §6 with a calculation of the relative likelihood per unit time for the emergence of life [11], which is of particular importance for studies attempting to gauge the level of fine-tuning required for the cosmological or fundamental physics parameters that would allow life to emerge in our Universe.

2 The Habitable Epoch of the Early Universe

2.1 Section Background

The habitable zone is commonly defined in reference to a distance from a luminous source, such as a star [1, 2], whose heat maintains the surface of a rocky planet at a temperature of $\sim 300\text{K}$, allowing liquid water to exist and the chemistry of “life as we know it” to operate. In the section, we point out that the cosmic microwave background (CMB) provided a uniform

heating source at a temperature of $T_{\text{cmb}} = 272.6\text{K} \times [(1+z)/100]$ [12] that could have made by itself rocky planets habitable at redshifts $(1+z) = 100\text{--}137$ in the early Universe, merely 10–17 million years after the Big Bang.

In order for rocky planets to exist at these early times, massive stars with tens to hundreds of solar masses, whose lifetime is much shorter than the age of the Universe, had to form and enrich the primordial gas with heavy elements through winds and supernova explosions [13, 14]. Indeed, numerical simulations predict that predominantly massive stars have formed in the first halos of dark matter to collapse [5, 15]. For massive stars that are dominated by radiation pressure and shine near their Eddington luminosity $L_{\text{E}} = 1.3 \times 10^{40} \text{ erg s}^{-1} (m/100M_{\odot})$, the lifetime is independent of stellar mass m and set by the 0.7% nuclear efficiency for converting rest mass to radiation, $\sim (0.007mc^2)/L_{\text{E}} = 3 \text{ Myr}$ [16, 17]. We next examine how early did such stars form within the observable volume of our Universe.

2.2 First Planets

In the standard cosmological model, structure forms hierarchically – starting from small spatial scales, through the gravitational growth of primordial density perturbations [5]. On any given spatial scale R , the probability distribution of fractional density fluctuations δ is assumed to have a Gaussian form, $P(\delta)d\delta = (2\pi\sigma^2)^{-1/2} \exp\{-\delta^2/2\sigma^2\}d\delta$, with a *root-mean-square* amplitude $\sigma(R)$ that is initially much smaller than unity. The initial $\sigma(R)$ is tightly constrained on large scales, $R \gtrsim 1 \text{ Mpc}$, through observations of the CMB anisotropies and galaxy surveys [18, 19], and is extrapolated theoretically to smaller scales. Throughout the discussion, we normalize spatial scales to their so-called “comoving” values in the present-day Universe. The assumed Gaussian shape of $P(\delta)$ has so far been tested only on scales $R \gtrsim 1 \text{ Mpc}$ for $\delta \lesssim 3\sigma$ [20], but was not verified in the far tail of the distribution or on small scales that are first to collapse in the early Universe.

As the density in a given region rises above the background level, the matter in it detaches from the Hubble expansion and eventually collapses owing to its self-gravity to make a gravitationally bound (virialized) object like a galaxy. The abundance of regions that collapse and reach virial equilibrium at any given time depends sensitively on both $P(\delta)$ and $\sigma(R)$. Each collapsing region includes a mix of dark matter and ordinary matter (often labeled as “baryonic”). If the baryonic gas is able to cool below the virial temperature inside the dark matter halo, then it could fragment into dense clumps and make stars.

At redshifts $z \gtrsim 140$ Compton cooling on the CMB is effective on a timescale comparable to the age of the Universe, given the residual fraction of free electrons left over from cosmological recombination (see §2.2 in Ref. [5] and also Ref. [21]). The thermal coupling to the CMB tends to bring the gas temperature to T_{cmb} , which at $z \sim 140$ is similar to the temperature floor associated with molecular hydrogen cooling [22–24]. In order for virialized gas in a dark matter halo to cool, condense and fragment into stars, the halo virial temperature T_{vir} has to exceed $T_{\text{min}} \approx 300\text{K}$, corresponding to T_{cmb} at $(1+z) \sim 110$. This implies a halo mass in excess of $M_{\text{min}} = 10^4 M_{\odot}$, corresponding to a baryonic mass $M_{\text{b,min}} = 1.5 \times 10^3 M_{\odot}$, a circular virial velocity $V_{\text{c,min}} = 2.6 \text{ km s}^{-1}$ and a virial radius $r_{\text{vir,min}} = 6.3 \text{ pc}$ (see §3.3 in Ref. [5]). This value of M_{min} is close to the minimum halo mass to assemble baryons at that redshift (see §3.2.1 in Ref. [5] and Fig. 2 of Ref. [25]).

The corresponding number of star-forming halos on our past light cone is given by [7],

$$N = \int_{(1+z)=100}^{(1+z)=137} n(M > M_{\text{min}}, z') \frac{dV}{dz'} dz', \quad (2.1)$$

where $n(M > M_{\min})$ is the comoving number density of halos with a mass $M > M_{\min}$ [26], and $dV = 4\pi r^2 dr$ is the comoving volume element with $dr = cdt/a(t)$. Here, $a(t) = (1+z)^{-1}$ is the cosmological scale factor at time t , and $r(z) = c \int_0^z dz'/H(z')$ is the comoving distance. The Hubble parameter for a flat Universe is $H(z) \equiv (\dot{a}/a) = H_0 \sqrt{\Omega_m(1+z)^3 + \Omega_r(1+z)^4 + \Omega_\Lambda}$, with Ω_m , Ω_r and Ω_Λ being the present-day density parameters of matter, radiation and vacuum, respectively. The total number of halos that existed at $(1+z) \sim 100$ within our entire Hubble volume (not restricted to the light cone), $N_{\text{tot}} \equiv n(M > M_{\min}, z = 99) \times (4\pi/3)(3c/H_0)^3$, is larger than N by a factor of $\sim 10^3$.

For the standard cosmological parameters [18], we find that the first star-forming halos on our past light cone reached its maximum turnaround radius¹ (with a density contrast of 5.6) at $z \sim 112$ and collapsed (with an average density contrast of 178) at $z \sim 71$. Within the entire Hubble volume, a turnaround at $z \sim 122$ resulted in the first collapse at $z \sim 77$. This result includes the delay by $\Delta z \sim 5.3$ expected from the streaming motion of baryons relative to the dark matter [6].

The above calculation implies that rocky planets could have formed within our Hubble volume by $(1+z) \sim 78$ but not by $(1+z) \sim 110$ if the initial density perturbations were perfectly Gaussian. However, the host halos of the first planets are extremely rare, representing just $\sim 2 \times 10^{-17}$ of the cosmic matter inventory. Since they lie ~ 8.5 standard deviations (σ) away on the exponential tail of the Gaussian probability distribution of initial density perturbations, $P(\delta)$, their abundance could have been significantly enhanced by primordial non-Gaussianity [27–29] if the decline of $P(\delta)$ at high values of δ/σ is shallower than exponential. The needed level of deviation from Gaussianity is not ruled out by existing data sets [30]. Non-Gaussianity below the current limits is expected in generic models of cosmic inflation [31] that are commonly used to explain the initial density perturbations in the Universe.

2.3 Section Summary and Implications

We highlighted a new regime of habitability made possible for ~ 6.6 Myr by the uniform CMB radiation at redshifts $(1+z) = 100$ –137, just when the first generation of star-forming halos (with a virial mass $\gtrsim 10^4 M_\odot$) turned around in the standard cosmological model with Gaussian initial conditions. Deviations from Gaussianity in the far (8.5σ) tail of the probability distribution of initial density perturbations, could have led already at these redshifts to the birth of massive stars, whose heavy elements triggered the formation of rocky planets with liquid water on their surface.²

Thermal gradients are needed for life. These can be supplied by geological variations on the surface of rocky planets. Examples for sources of free energy are geothermal energy powered by the planet’s gravitational binding energy at formation and radioactive energy from unstable elements produced by the earliest supernova. These internal heat sources (in addition to possible heating by a nearby star), may have kept planets warm even without the CMB, extending the habitable epoch from $z \sim 100$ to later times. The lower CMB temperature at late times may have allowed ice to form on objects that delivered water to a

¹In the spherical collapse model, the turnaround time is half the collapse time.

²The dynamical time of galaxies is shorter than $\sim 1/\sqrt{200} = 7\%$ of the age of the Universe at any redshift since their average density contrast is $\gtrsim 200$. After the first stars formed, the subsequent delay in producing heavy elements from the first supernovae could have been as short as a few Myr. The supernova ejecta could have produced high-metallicity islands that were not fully mixed with the surrounding primordial gas, leading to efficient formation of rocky planets within them.

planet’s surface, and helped to maintain the cold trap of water in the planet’s stratosphere. Planets could have kept a blanket of molecular hydrogen that maintained their warmth [32, 33], allowing life to persist on internally warmed planets at late cosmic times. If life persisted at $z \lesssim 100$, it could have been transported to newly formed objects through panspermia. Under the assumption that interstellar panspermia is plausible, the redshift of $z \sim 100$ can be regarded as the earliest cosmic epoch after which life was possible in our Universe.

The feasibility of life in the early universe can be tested by searching for planets with atmospheric biosignatures around low-metallicity stars in the Milky Way galaxy or its dwarf galaxy satellites. Such stars represent the closest analogs to the first generation of stars at early cosmic times.

The possibility that the chemistry of life could have started in our universe only 10–17 Myr after the Big Bang argues against the anthropic explanation³ for the value of the cosmological constant [34], especially if the characteristic amplitude of initial density perturbations or the level of non-Gaussianity is allowed to vary in different regions of the multiverse⁴ [35, 36]. In principle, the habitable cosmological epoch considered here allows for life to emerge in a Universe with a cosmological constant that is $(1+z)^3 \sim 10^6$ times bigger than observed [10]. If observers can eventually emerge from primitive forms of life at an arbitrarily later time in such a Universe, then their existence would be in conflict with the anthropic reasoning for the low value of the cosmological constant in our Universe. Even when placed on a logarithmic scale, the corresponding discrepancy in the vacuum energy density is substantial, spanning $\sim 5\%$ of the ~ 120 orders of magnitude available up to the Planck density. The volume associated with inflating regions of larger vacuum density is exponentially greater than our region, making residence in them far more likely.

3 CEMP stars: possible hosts to carbon planets in the early universe

3.1 Section Background

The questions of when, where, and how the first planetary systems formed in cosmic history remain crucial to our understanding of structure formation and the emergence of life in the early Universe [3]. In the Cold Dark Matter model of hierarchical structure formation, the first stars are predicted to have formed in dark matter haloes that collapsed at redshifts $z \lesssim 70$, about 30 million years after the Big Bang [5, 15, 36–38]. These short-lived, metal-free, massive first-generation stars ultimately exploded as supernovae (SNe) and enriched the interstellar medium (ISM) with the heavy elements fused in their cores. The enrichment of gas with metals that had otherwise been absent in the early Universe enabled the formation of the first low-mass stars, and perhaps, marked the point at which star systems could begin to form planets [39–41]. In the core accretion model of planet formation (e.g. [42, 43]), elements heavier than hydrogen and helium are necessary not only to form the dust grains that are the building blocks of planetary cores, but to extend the lifetime of the protostellar disk long enough to allow the dust grains to grow via merging and accretion to form planetesimals [44–47].

³In difference from Ref. [34], we require here that stars form in any low-mass halo rather than in a galaxy as massive as the Milky-Way, as the pre-requisite for life.

⁴An increase in the initial amplitude of density perturbations on the mass scale of $10^4 M_\odot$ by a modest factor of $1.4 \times [(1+z)/110]$ would have enabled star formation within the Hubble volume at redshifts $(1+z) > 110$ even for perfectly Gaussian initial conditions.

In the past four decades, a broad search has been launched for low-mass Population II stars in the form of extremely metal-poor sources within the halo of the Galaxy. The HK survey [48], the Hamburg/ESO Survey [49, 50], the Sloan Digital Sky Survey (SDSS; [51]), and the SEGUE survey [52] have all significantly enhanced the sample of metal-poor stars with $[\text{Fe}/\text{H}] < -2.0$. Although these iron-poor stars are often referred to in the literature as “metal-poor” stars, it is critical to note that $[\text{Fe}/\text{H}]$ does not necessarily reflect a stellar atmosphere’s total metal content. The equivalence between “metal-poor” and “Fe-poor” appears to fall away for stars with $[\text{Fe}/\text{H}] < -3.0$ since many of these stars exhibit large overabundances of elements such as C, N, and O; the total mass fractions, Z , of the elements heavier than He are therefore not much lower than the solar value in these iron-poor stars.

Carbon-enhanced metal-poor (CEMP) stars comprise one such chemically anomalous class of stars, with carbon-to-iron ratios $[\text{C}/\text{Fe}] \geq 0.7$ (as defined in [53–55]). The fraction of sources that fall into this category increases from $\sim 15\text{--}20\%$ for stars with $[\text{Fe}/\text{H}] < -2.0$, to 30% for $[\text{Fe}/\text{H}] < -3.0$, to $\sim 75\%$ for $[\text{Fe}/\text{H}] < -4.0$ [55–57]. Furthermore, the degree of carbon enhancement in CEMP stars has been shown to notably increase as a function of decreasing metallicity, rising from $[\text{C}/\text{Fe}] \sim 1.0$ at $[\text{Fe}/\text{H}] = -1.5$ to $[\text{C}/\text{Fe}] \sim 1.7$ at $[\text{Fe}/\text{H}] = -2.7$. [54]. Given the significant frequency and level of carbon-excess in this subset of metal-poor Population II stars, the formation of carbon planets around CEMP stars in the early universe presents itself as an intriguing possibility.

From a theoretical standpoint, the potential existence of carbon exoplanets, consisting of carbides and graphite instead of Earth-like silicates, has been suggested by Ref. [58]. Using the various elemental abundances measured in planet-hosting stars, subsequent works have sought to predict the corresponding variety of terrestrial exoplanet compositions expected to exist [59–61]. Assuming that the stellar abundances are similar to those of the original circumstellar disk, related simulations yield planets with a whole range of compositions, including some that are almost exclusively C and SiC; these occur in disks with $\text{C}/\text{O} > 0.8$, favorable conditions for carbon condensation [62]. Observationally, there have also been indications of planets with carbon-rich atmospheres, e.g. WASP-12b [63], and carbon-rich interiors, e.g. 55 Cancri e [64].

In this section, we explore the possibility of carbon planet formation around the iron-deficient, but carbon-rich subset of low-mass stars, mainly, CEMP stars. Standard definitions of elemental abundances and ratios are adopted. For element X, the logarithmic absolute abundance is defined as the number of atoms of element X per 10^{12} hydrogen atoms, $\log \epsilon(\text{X}) = \log_{10}(N_{\text{X}}/N_{\text{H}}) + 12.0$. For elements X and Y, the logarithmic abundance ratio relative to the solar ratio is defined as $[\text{X}/\text{Y}] = \log_{10}(N_{\text{X}}/N_{\text{Y}}) - \log_{10}(N_{\text{X}}/N_{\text{Y}})_{\odot}$. The solar abundance set is that of Ref. [65], with a solar metallicity $Z_{\odot} = 0.0134$.

3.2 Star-forming environment of CEMP stars

A great deal of effort has been directed in the literature towards understanding theoretically, the origin of the most metal-poor stars, and in particular, the large fraction that is C-rich. These efforts have been further perturbed by the fact that CEMP stars do not form a homogenous group, but can rather be further subdivided into two main populations [56]: carbon-rich stars that show an excess of heavy neutron-capture elements (CEMP-s, CEMP-r, and CEMP-r/s), and carbon-rich stars with a normal pattern of the heavy elements (CEMP-no). In the following sections, we focus on stars with $[\text{Fe}/\text{H}] \leq -3.0$, which have been shown to fall almost exclusively in the CEMP-no subset [66].

A number of theoretical scenarios have been proposed to explain the observed elemental abundances of these stars, though there is no universally accepted hypothesis. The most extensively studied mechanism to explain the origin of CEMP-no stars is the mixing and fallback model, where a “faint” Population III SN explodes, but due to a relatively low explosion energy, only ejects its outer layers, rich in lighter elements (up to magnesium); its innermost layers, rich in iron and heavier elements, fall back onto the remnant and are not recycled in the ISM [67, 68]. This potential link between primeval SNe and CEMP-no stars is supported by recent studies which demonstrate that the observed ratio of carbon-enriched to carbon-normal stars with $[\text{Fe}/\text{H}] < -3.0$ is accurately reproduced if SNe were the main source of metal-enrichment in the early Universe [69, 70]. Furthermore, the observed abundance patterns of CEMP-no stars have been found to be generally well matched by the nucleosynthetic yields of primordial faint SNe [68, 71–79]. These findings suggest that most of the CEMP-no stars were probably born out of gas enriched by massive, first-generation stars that ended their lives as Type II SNe with low levels of mixing and a high degree of fallback.

Under such circumstances, the gas clouds which collapse and fragment to form these CEMP-no stars and their protostellar disks may contain significant amounts of carbon dust grains. Observationally, dust formation in SNe ejecta has been inferred from isotopic anomalies in meteorites where graphite, SiC, and Si_3N_4 dust grains have been identified as SNe condensates [80]. Furthermore, in situ dust formation has been unambiguously detected in the expanding ejecta of SNe such as SN 1987A [81, 82] and SN 1999em [83]. The existence of cold dust has also been verified in the supernova remnant of Cassiopeia A by SCUBA’s recent submillimeter observations, and a few solar masses worth of dust is estimated to have condensed in the ejecta [84].

Theoretical calculations of dust formation in primordial core-collapsing SNe have demonstrated the condensation of a variety of grain species, starting with carbon, in the ejecta, where the mass fraction tied up in dust grains grows with increasing progenitor mass [85–87]. Ref. [76, 77] consider, in particular, dust formation in weak Population III SNe ejecta, the type believed to have polluted the birth clouds of CEMP-no stars. Tailoring the SN explosion models to reproduce the observed elemental abundances of CEMP-no stars, they find that: (i) for all the progenitor models investigated, amorphous carbon (AC) is the only grain species that forms in significant amounts; this is a consequence of extensive fallback, which results in a distinct, carbon-dominated ejecta composition with negligible amounts of other metals, such as Mg, Si, and Al, that can enable the condensation of alternative grain types; (ii) the mass of carbon locked into AC grains increases when the ejecta composition is characterized by an initial mass of C greater than the O mass; this is particularly true in zero metallicity supernova progenitors, which undergo less mixing than their solar metallicity counterparts [72]; in their stratified ejecta, C-grains are found only to form in layers where $\text{C}/\text{O} > 1$; in layers where $\text{C}/\text{O} < 1$, all the carbon is promptly locked in CO molecules; (iii) depending on the model, the mass fraction of dust (formed in SNe ejecta) that survives the passage of a SN reverse shock ranges between 1 to 85%; this fraction is referred to as the carbon condensation efficiency; (iv) further grain growth in the collapsing birth clouds of CEMP-no stars, due to the accretion of carbon atoms in the gas phase onto the remaining grains, occurs only if $\text{C}/\text{O} > 1$ and is otherwise hindered by the formation of CO molecules.

Besides the accumulation of carbon-rich grains imported from the SNe ejecta, Fischer-Tropsch-type reactions (FTTs) may also contribute to solid carbon enrichment in the protostellar disks of CEMP-no stars by enabling the conversion of nebular CO and H_2 to other

forms of carbon [88]. Furthermore, in carbon-rich gas, the equilibrium condensation sequence changes significantly from the sequence followed in solar composition gas where metal oxides condense first. In nebular gas with $C/O \gtrsim 1$, carbon-rich compounds such as graphite, carbides, nitrides, and sulfides are the highest temperature condensates ($T \approx 1200\text{--}1600\text{ K}$) [62]. Thus, if planet formation is to proceed in this C-rich gas, the protoplanetary disks of these CEMP-no stars may spawn many carbon planets.

3.3 Orbital Radii of Potential Carbon Planets

Given the significant abundance of carbon grains, both imported from SNe ejecta and produced by equilibrium and non-equilibrium mechanisms operating in the C-rich protoplanetary disks, the emerging question is: would these dust grains have enough time to potentially coagulate and form planets around their host CEMP-no stars?

In the core accretion model, terrestrial planet formation is a multi-step process, starting with the aggregation and settling of dust grains in the protoplanetary disk [42, 43, 89–92]. In this early stage, high densities in the disk allow particles to grow from submicron-size to meter-size through a variety of collisional processes including Brownian motion, settling, turbulence, and radial migration. The continual growth of such aggregates by coagulation and sticking eventually leads to the formation of kilometer-sized planetesimals, which then begin to interact gravitationally and grow by pairwise collisions, and later by runaway growth [89]. In order for terrestrial planets to ultimately form, these processes must all occur within the lifetime of the disk itself, a limit which is set by the relevant timescale of the physical phenomena that drive disk dissipation.

A recent study by Ref. [46] of clusters in the Extreme Outer Galaxy (EOG) provides observational evidence that low-metallicity disks have shorter lifetimes ($< 1\text{ Myr}$) compared to solar metallicity disks ($\sim 5\text{--}6\text{ Myr}$). This finding is consistent with models in which photoevaporation by energetic (ultraviolet or X-ray) radiation of the central star is the dominant disk dispersal mechanism. While the opacity source for EUV (extreme-ultraviolet) photons is predominantly hydrogen and is thus metallicity-independent, X-ray photons are primarily absorbed by heavier elements, mainly carbon and oxygen, in the inner gas and dust shells. Therefore, in low metallicity environments where these heavy elements are not abundant and the opacity is reduced, high density gas at larger columns can be ionized and will experience a photoevaporative flow if heated to high enough temperatures [47, 93].

Assuming that photoevaporation is the dominant mechanism through which circumstellar disks lose mass and eventually dissipate, we adopt the metallicity-dependent disk lifetime, derived in Ref. [47] using X-ray+EUV models [94],

$$t_{\text{disk}} \propto Z^{0.77(4-2p)/(5-2p)} \quad (3.1)$$

where Z is the total metallicity of the disk and p is the power-law index of the disk surface density profile ($\Sigma \propto r^{-p}$). A mean power-law exponent of $p \sim 0.9$ is derived by modeling the spatially resolved emission morphology of young stars at (sub)millimeter wavelengths [95, 96] and the timescale is normalized such that the mean lifetime for disks of solar metallicity is 2 Myr [47]. Thus the disk lifetime, is dominated by carbon dust grains in the CEMP-no stars considered here, we adopt the carbon abundance relative to solar $[C/H]$ as a proxy for the overall metallicity Z . We adopt the carbon abundance relative to solar $[C/H]$ as a proxy for the overall metallicity Z since the opacity, which largely determines the photoevaporation rate, and thus the disk lifetime, is dominated by carbon dust grains in the CEMP-no stars we consider in this work.

The timescale for planet formation is believed to be effectively set by the time it takes dust grains to settle into the disk midplane. The subsequent process of runaway planetesimal formation, possibly occurring via a series of pairwise collisions, must be quick, since otherwise, the majority of the solid disk material would radially drift towards the host star and evaporate in the hot inner regions of the circumstellar disk [92]. We adopt the one-particle model of Ref. [97] to follow the mass growth of dust grains via collisions as they fall through and sweep up the small grains suspended in the disk. Balancing the gravitational force felt by a small dust particle at height z above the mid-plane of a disk with the aerodynamic drag (in the Epstein regime) gives a dust settling velocity of

$$v_{sett} = \frac{dz}{dt} = \frac{3\Omega_K^2 z m}{4\rho c_s \sigma_d} \quad (3.2)$$

where $\sigma_d = \pi a^2$ is the cross-section of the dust grain with radius a and $c_s = \sqrt{k_B T(r)/\mu m_H}$ is the isothermal sound speed with m_H being the mass of a hydrogen atom and $\mu=1.36$ being the mean molecular weight of the gas (including the contribution of helium). $\Omega_K = \sqrt{GM_*/r^3}$ is the Keplerian velocity of the disk at a distance r from the central star of mass M_* , which we take to be $M_* = 0.8 M_\odot$ as representative of the low-masses associated with CEMP-no stars [57, 98]. The disk is assumed to be in hydrostatic equilibrium with a density given by

$$\rho(z, r) = \frac{\Sigma(r)}{h\sqrt{2\pi}} \exp\left(-\frac{z^2}{2h^2}\right) \quad (3.3)$$

where the disk scale height is $h = c_s/\Omega_K$. For the disk surface density $\Sigma(r)$ and temperature $T(r)$ profiles, we adopt the radial power-law distributions fitted to (sub-)millimeter observations of circumstellar disks around young stellar objects [95, 96, 99],

$$T(r) = 200 \text{ K} \left(\frac{r}{1 \text{ AU}}\right)^{-0.6} \quad (3.4)$$

$$\Sigma(r) = 10^3 \text{ g/cm}^2 \left(\frac{r}{1 \text{ AU}}\right)^{-0.9}. \quad (3.5)$$

Although these relations were observationally inferred from disks with solar-like abundances, we choose to rely on them for our purposes given the lack of corresponding measurements for disks around stars with different abundance patterns.

The rate of grain growth, dm/dt , is determined by the rate at which grains, subject to small-scale Brownian motion, collide and stick together as they drift towards the disk mid-plane through a sea of smaller solid particles. If coagulation results from every collision, then the mass growth rate of a particle is effectively the amount of solid material in the volume swept out the particle's geometric cross-section,

$$\frac{dm}{dt} = f_{dg} \rho \sigma_d \left(v_{rel} + \frac{dz}{dt}\right) \quad (3.6)$$

where dz/dt is the dust settling velocity given by equation (2) and

$$v_{rel} = \sqrt{\frac{8k_B T(m_1 + m_2)}{\pi m_1 m_2}} \approx \sqrt{\frac{8k_B T}{\pi m}} \quad (3.7)$$

Table 1. Basic data^a for CEMP stars considered in this section

Star	$\log g^b$	[Fe/H]	[C/Fe]	C/O ^c	Source ^d
HE 0107-5240	2.2	-5.44	3.82	14.1	1,2
SDSS J0212+0137	4.0	-3.57	2.26	2.6	3
SDSS J1742+2531	4.0	-4.77	3.60	2.2	3
G 77-61	5.1	-4.03	3.35	12.0	4, 5
HE 2356-0410 ^e	2.65	-3.19	2.61	>14.1	6

^a Abundances based on one-dimensional LTE model-atmosphere analyses

^b Logarithm of the gravitational acceleration at the surface of stars expressed in cm s^{-2}

^c $\text{C/O} = N_{\text{C}}/N_{\text{O}} = 10^{[\text{C/O}] + \log \epsilon(\text{C})_{\odot} - \log \epsilon(\text{O})_{\odot}}$

^d **References:** (1) [101]; (2) [102]; (3) [79]; (4) [103]; (5) [104]; (6) [105].

^e CS 22957-027

is the relative velocity in the Brownian motion regime between grains with masses $m_1 = m_2 = m$. To calculate the dust-to-gas mass ratio in the disk f_{dg} , we follow the approach in Ref. [100] and relate two expressions for the mass fraction of C: (i) the fraction of carbon in the dust, $f_{dg} M_{C,dust}/M_{dust}$, where M_{dust} is the total dust mass and $M_{C,dust}$ is the carbon dust mass ; and (ii) the fraction of carbon in the gas, $\mu_C n_C/\mu n_H$, where μ_C is the molecular weight of carbon ($\sim 12m_p$) and n_C and n_H are the carbon and hydrogen number densities, respectively.

We then assume that a fraction f_{cond} (referred to from now on as the carbon condensation efficiency) of all the carbon present in the gas cloud is locked up in dust, such that

$$f_{cond} \frac{\mu_C n_C}{\mu n_H} = f_{dg} \frac{M_{C,dust}}{M_{dust}}. \quad (3.8)$$

Since faint Population III SNe are believed to have polluted the birth clouds of CEMP-no stars, and the only grain species that forms in non-negligible amounts in these ejecta is amorphous carbon [76, 77], we set $M_{dust} = M_{C,dust}$. Rewriting equation (8) in terms of abundances relative to the Sun, we obtain

$$f_{dg} = f_{cond} \frac{\mu_C}{\mu} 10^{[\text{C/H}] + \log \epsilon(\text{C})_{\odot} - 12} \quad (3.9)$$

where $\log \epsilon(\text{C})_{\odot} = 8.43 \pm 0.05$ [65] is the solar carbon abundance.

For a specified metallicity $[\text{C/H}]$ and radial distance r from the central star, we can then estimate the time it takes for dust grains to settle in the disk by integrating equations (2) and (6) from an initial height of $z(t=0) = 4h$ with an initial dust grain mass of $m(t=0) = 4\pi a_{init}^3 \rho_d/3$. The specific weight of dust is set to $\rho_d = 2.28 \text{ g cm}^{-3}$, reflecting the material density of carbon grains expected to dominate the circumstellar disks of CEMP-no stars. The initial grain size a_{init} is varied between 0.01 and 1 μm to reflect the range of characteristic radii of carbon grains found when modeling CEMP-no star abundance patterns [76]. Comparing the resulting dust-settling timescale to the disk lifetime given by equation (1) for the specified metallicity, we can then determine whether there is enough time for carbon

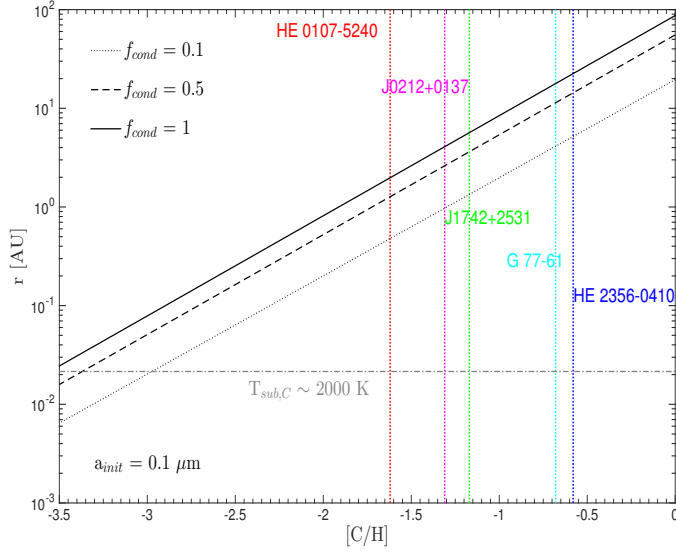


Figure 1. The maximum distance r_{max} from the host star out to which planetesimal formation is possible as a function of the star’s metallicity, expressed as the carbon abundance relative to that of the Sun, $[C/H]$. The dotted, dashed, and solid black curves correspond to the results obtained assuming carbon condensation efficiencies of 10%, 50%, and 100%, respectively, and an initial grain size of $a_{init} = 0.1 \mu\text{m}$. The gray dash-dotted curve corresponds to the distance at which the disk temperature approaches the sublimation temperature of carbon dust grains, $T_{sub,C} \sim 2000 \text{ K}$; the formation of carbon planetesimals will therefore be suppressed at distances that fall below this line, $r \lesssim 0.02 \text{ AU}$. The colored vertical lines represent various observed CEMP stars with measured carbon abundances, $[C/H]$.

dust grains to settle in the mid-plane of the disk and there undergo runaway planetesimal formation before the disk is dissipated by photoevaporation. For the purposes of this simple model, we neglected possible turbulence in the disk which may counteract the effects of vertical settling, propelling particles to higher altitudes and thus preventing them from fully settling into the disk mid-plane [92]. We have also not accounted for the effects of radial drift, which may result in the evaporation of solid material in the hot inner regions of the circumstellar disk.

As the dust settling timescale is dependent on the disk surface density $\Sigma(r)$ and temperature $T(r)$, we find that for a given metallicity, $[C/H]$, there is a maximum distance r_{max} from the central star out to which planetesimal formation is possible. At larger distances from the host star, the dust settling timescale exceeds the disk lifetime and so carbon planets with semi-major axes $r > r_{max}$ are not expected to form. A plot of the maximum semi-major axis expected for planet formation around a CEMP-no star as a function of the carbon abundance relative to the Sun $[C/H]$ is shown in Figure 3.3 for carbon condensation efficiencies ranging between $f_{cond} = 0.1$ and 1. As discovered in Ref. [106] where the critical iron abundance for terrestrial planet formation is considered as a function of the distance from the host star, we find a linear relation between $[C/H]$ and r_{max} ,

$$[C/H] = \log \left(\frac{r_{max}}{1 \text{ AU}} \right) - \alpha \quad (3.10)$$

where $\alpha = 1.3, 1.7$, and 1.9 for $f_{cond} = 0.1, 0.5$, and 1 , respectively, assuming an initial grain size of $a_{init} = 0.1 \mu\text{m}$. These values for α change by less than 1% for smaller initial grain sizes, $a_{init} = 0.01 \mu\text{m}$, and by no more than 5% for larger initial grain sizes $a_{init} = 1 \mu\text{m}$; given this weak dependence on a_{init} , we only show our results for a single initial grain size of $a_{init} = 0.1 \mu\text{m}$. The distance from the host star at which the temperature of the disk approaches the sublimation temperature of carbon dust, $T_{sub,C} \sim 2000 \text{ K}$ [107], is depicted as well (dash-dotted gray curve). At distances closer to the central star than $r \simeq 0.02 \text{ AU}$, temperatures well exceed the sublimation temperature of carbon grains; grain growth and subsequent carbon planetesimal formation are therefore quenched in this inner region.

Figure 3.3 shows lines representing various observed CEMP stars with measured carbon abundances, mainly, HE 0107-5240 [98, 101], SDSS J0212+0137 [79], SDSS J1742+2531 [79], G 77-61 [103, 104, 108], and HE 2356-0410 [105, 109]. These stars all have iron abundances (relative to solar) $[\text{Fe}/\text{H}] < -3.0$, carbon abundances (relative to solar) $[\text{C}/\text{Fe}] > 2.0$, and carbon-to-oxygen ratios $\text{C}/\text{O} > 1$. This latter criteria maximizes the abundance of solid carbon available for planet formation in the circumstellar disks by optimizing carbon grain growth both in stratified SNe ejecta and later, in the collapsing molecular birth clouds of these stars. It also advances the possibility of carbon planet formation by ensuring that planet formation proceeds by a carbon-rich condensation sequence in the protoplanetary disk. SDSS J0212+0137 and HE 2356-0410 have both been classified as CEMP-no stars, with measured barium abundances $[\text{Ba}/\text{Fe}] < 0$ (as defined in [56]); the other three stars are Ba-indeterminate, with only high upper limits on $[\text{Ba}/\text{Fe}]$, but are believed to belong to the CEMP-no subclass given their light-element abundance patterns. The carbon abundance, $[\text{C}/\text{H}]$, dominates the total metal content of the stellar atmosphere in these five CEMP objects, contributing more than 60% of the total metallicity in these stars. A summary of the relevant properties of the CEMP stars considered in this analysis can be found in Table 1. We find that carbon planets may be orbiting iron-deficient stars with carbon abundances $[\text{C}/\text{H}] \sim -0.6$, such as HE 2356-0410, as far out as $\sim 20 \text{ AU}$ from their host star in the case where $f_{cond} = 1$. Planets forming around stars with less carbon enhancement, i.e. HE 0107-5240 with $[\text{C}/\text{H}] \sim -1.6$, are expected to have more compact orbits, with semi-major axes $r < 2 \text{ AU}$. If the carbon condensation efficiency is only 10%, the expected orbits grow even more compact, with maximum semi-major axes of ~ 5 and 0.5 AU , respectively.

3.4 Mass-Radius Relationship for Carbon Planets

Next we present the relationship between the mass and radius of carbon planets that we have shown may theoretically form around CEMP-no stars. These mass-radius relations have already been derived in the literature for a wide range of rocky and icy exoplanet compositions [110–114]. Here, we follow the approach of Ref. [110] and solve the three canonical equations of internal structure for solid planets,

1. mass conservation

$$\frac{dm(r)}{dr} = 4\pi r^2 \rho(r), \quad (3.11)$$

2. hydrostatic equilibrium

$$\frac{dP(r)}{dr} = -\frac{Gm(r)\rho(r)}{r^2}, \text{ and} \quad (3.12)$$

3. the equation of state (EOS)

$$P(r) = f(\rho(r), T(r)), \quad (3.13)$$

where $m(r)$ is the mass contained within radius r , $P(r)$ is the pressure, $\rho(r)$ is the density of the spherical planet, and f is the unique equation of state (EOS) of the material of interest, in this case, carbon.

Carbon grains in circumstellar disks most likely experience many shock events during planetesimal formation which may result in the modification of their structure. The coagulation of dust into clumps, the fragmentation of the disk into clusters of dust clumps, the merging of these clusters into ~ 1 km planetesimals, the collision of planetesimals during the accretion of meteorite parent bodies, and the subsequent collision of the parent bodies after their formation all induce strong shock waves that are expected to chemically and physically alter the materials. Subject to these high temperatures and pressures, the amorphous carbon grains polluting the protoplanetary disks around CEMP stars are expected to undergo graphitization and may even crystallize into diamond [115–117]. In our calculations, the equation of state at low pressures, $P \leq 14$ GPa, is set to the third-order finite strain Birch-Murnaghan EOS (BME; [118]) for graphite,

$$P = \frac{3}{2}K_0 \left(\eta^{7/3} - \eta^{5/3} \right) \left[1 + \frac{3}{4} \left(K'_0 - 4 \right) \left(\eta^{2/3} - 1 \right) \right] \quad (3.14)$$

where $\eta = \rho/\rho_0$ is the compression ratio with respect to the ambient density, ρ_0 , K_0 is the bulk modulus of the material, and K'_0 is the pressure derivative. Empirical fits to experimental data yields a BME EOS of graphite ($\rho_0 = 2.25 \text{ g cm}^{-3}$) with parameters $K_0 = 33.8$ GPa and $K'_0 = 8.9$ [119]. At 14 GPa, we incorporate the phase transition from graphite to diamond [119, 120] and adopt the Vinet EOS [121, 122],

$$P = 3K_0\eta^{2/3} \left(1 - \eta^{-1/3} \right) \exp \left[\frac{3}{2} \left(K'_0 - 1 \right) \left(1 - \eta^{-1/3} \right) \right] \quad (3.15)$$

with $K_0 = 444.5$ GPa and $K'_0 = 4.18$ empirically fit for diamond, $\rho_0 = 3.51 \text{ g cm}^{-3}$ [123]. (As pointed out in Ref. [114], the BME EOS is not fit to be extrapolated to high pressures since it is derived by expanding the elastic potential energy as a function of pressure keeping only the lowest order terms.) Finally, at pressures $P \gtrsim 1300$ GPa where electron degeneracy becomes increasingly important, we use the Thomas-Fermi-Dirac (TFD) theoretical EOS ([124]; equations (40)-(49)), which intersects the diamond EOS at $P \sim 1300$ GPa. Given that the full temperature-dependent carbon EOSs are either undetermined or dubious at best, all three EOSs adopted in this section are room-temperature EOSs for the sake of practical simplification.

Using a fourth-order Runge-Kutta scheme, we solve the system of equations simultaneously, numerically integrating equations (11) and (12) beginning at the planet's center with the inner boundary conditions $M(r=0) = 0$ and $P(r=0) = P_{\text{central}}$, where P_{central} is the central pressure. The outer boundary condition $P(r=R_p) = 0$ then defines the planetary radius R_p and total planetary mass $M_p = m(r=R_p)$. Integrating these equations for a range of P_{central} , with the appropriate EOS, $P = P(\rho)$, to close the system of equations, yields the mass-radius relationship for a given composition. We show this mass-radius relation for a purely solid carbon planet in Figure 3.4. We find that for masses $M_p \lesssim 800 M_{\oplus}$, gravitational forces are small compared with electrostatic Coulomb forces in hydrostatic equilibrium and so the planet's radius increases with increasing mass, $R_p \propto M_p^{1/3}$. However, at larger masses, the electrons are pressure-ionized and the resulting degeneracy pressure becomes significant, causing the planet radius to become constant and even decrease for increasing mass, $R_p \propto M_p^{-1/3}$ [125]. Planets which fall within the mass range $500 \lesssim M_p \lesssim 1300 M_{\oplus}$,

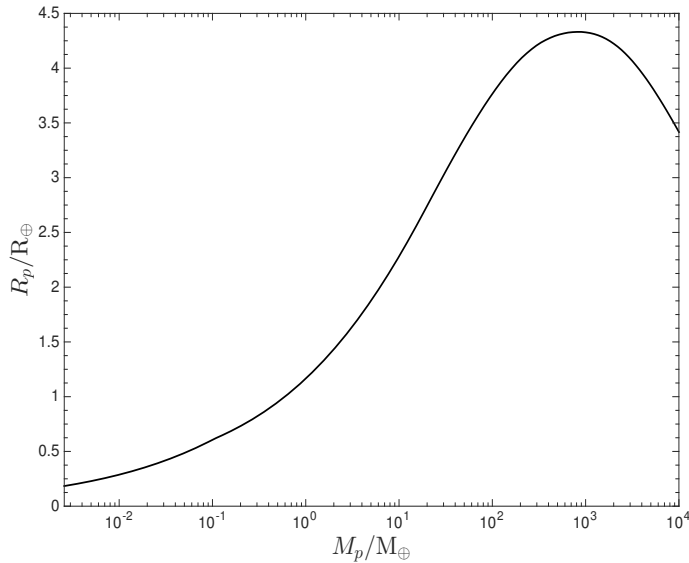


Figure 2. Mass-radius relation for solid homogenous, pure carbon planet

where the competing effects of Coulomb forces and electron degeneracy pressure cancel each other out, are expected to be approximately the same size, with $R_p \simeq 4.3 R_\oplus$, the maximum radius of a solid carbon planet. (In the case of gas giants, the planet radius can increase due to accretion of hydrogen and helium.)

Although the mass-radius relation illustrated in Figure 3.4 may alone not be enough to confidently distinguish a carbon planet from a water or silicate planet, the unique spectral features in the atmospheres of these carbon planets may provide the needed fingerprints. At high temperatures ($T \gtrsim 1000$ K), the absorption spectra of massive ($M \sim 10 - 60 M_\oplus$) carbon planets are expected to be dominated by CO, in contrast with the H₂O-dominated spectra of hot massive planets with solar-composition atmospheres [58]. The atmospheres of low-mass ($M \lesssim 10 M_\oplus$) carbon planets are also expected to be differentiable from their solar-composition counterparts due to their abundance of CO and CH₄, and lack of oxygen-rich gases like CO₂, O₂, and O₃ [58]. Furthermore, carbon planets of all masses at low temperatures are expected to accommodate hydrocarbon synthesis in their atmospheres; stable long-chain hydrocarbons are therefore another signature feature that can help observers distinguish the atmospheres of cold carbon planets and more confidently determine the bulk composition of a detected planet [58].

3.5 Transit Properties

The detection of theoretically proposed carbon planets around CEMP stars will provide us with significant clues regarding how early planet formation may have started in the Universe. While direct detection of these extrasolar planets remains difficult given the low luminosity of most planets, techniques such as the transit method are often employed to indirectly spot exoplanets and determine physical parameters of the planetary system. When a planet “transits” in front of its host star, it partially occludes the star and causes its’ observed brightness to drop by a minute amount. If the host star is observed during one of these transits, the resulting dip in its measured light curve can yield information regarding the relevant sizes of

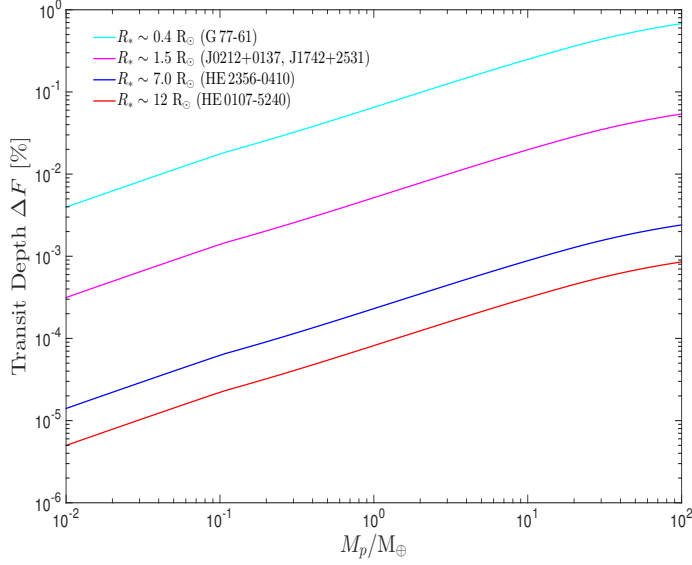


Figure 3. Transit depth as a function of the planetary mass (for a solid carbon planet transit) for different host stellar radii with an assumed stellar mass of $M_* = 0.8 M_\odot$. These particular stellar radii were chosen to correspond to the stellar radii of the CEMP stars considered in this section, mainly HE 0107-5240 (red), G 77-61 (cyan), HE 2356-0410 (blue), SDSS J0212+0137 and SDSS J1742+2531 (magenta), where the last two CEMP objects have the same measured surface gravity $\log g = 4.0$.

the star and the planet, the orbital semi-major axis, and the orbital inclination, among other characterizing properties.

A planetary transit across a star is characterized by three main parameters: the fractional change in the stellar brightness, the orbital period, and the duration of the transit [126]. The fractional change in brightness is referred to as the transit depth, ΔF (with a total observed flux F), and is simply defined as the ratio of the planet’s area to the host star’s area [127],

$$\Delta F = \frac{F_{\text{no transit}} - F_{\text{transit}}}{F_{\text{no transit}}} = \left(\frac{R_p}{R_*} \right)^2. \quad (3.16)$$

Given the stellar radius R_* , measurements of the relative flux change ΔF yield estimates of the size of the planet R_p , and the corresponding planetary mass M_p if the mass-radius relation for the planet is known. Using the R_p - M_p relation derived in §4, we illustrate in Figure 3.5 how the transit depth varies as a function of planetary mass in the case where a pure carbon planet transits across the face of its host CEMP star. Curves are shown for each of the five CEMP stars considered here, where we assume a stellar mass of $M_* = 0.8 M_\odot$ (representative of the low masses associated with old, iron-poor stellar objects) and derive the stellar radii using the stellar surface gravities g listed in Table 1, $R_* = \sqrt{GM_*/g}$.

As can be seen in Figure 3.5, the relative change in flux caused by an Earth-mass carbon planet transiting across its host CEMP star ranges from $\sim 0.0001\%$ for a host stellar radius of $R_* \sim 10 R_\odot$ to $\sim 0.01\%$ for a solar-sized stellar object. These shallow transit depths are thus expected to evade detection by ground-based transit surveys, which are generally limited in sensitivity to fractional flux changes on the order of 0.1% [128]. To push the limits of detection down to smaller, low-mass terrestrial planets requires space-based transit surveys

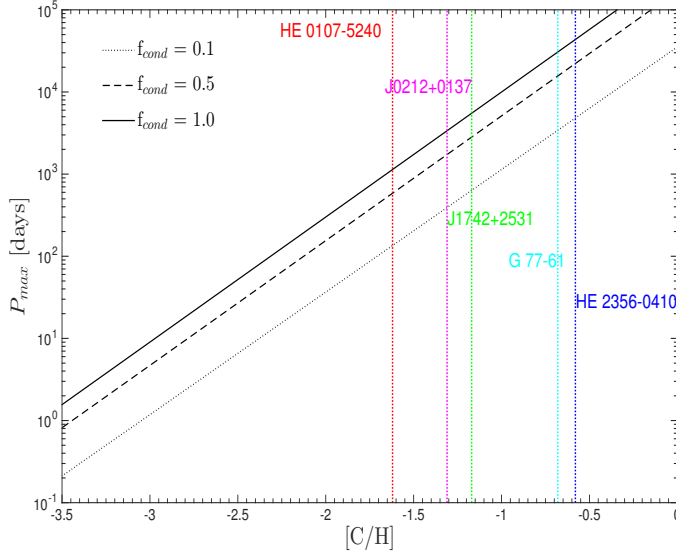


Figure 4. Maximum orbital period of a carbon planet transiting across its host CEMP star as a function of the star’s metallicity, expressed as the carbon abundance relative to that of the Sun, $[C/H]$. The dotted, dashed, and solid black curves denote the results obtained assuming carbon condensation efficiencies of 10%, 50%, and 100% in the parent CEMP star with mass $M_* = 0.8 M_\odot$. The colored vertical lines represent the five CEMP stars considered here with measured carbon abundances $[C/H]$.

that continuously monitor a large number of potential host stars over several years and measure their respective transit light curves. There are a number of ongoing, planned, and proposed space missions committed to this cause, including CoRoT (COnvection ROtation and planetary Transits), Kepler, PLATO (PLAnetary Transits and Oscillations of stars), TESS (Transiting Exoplanet Survey Satellite), and ASTrO (All Sky Transit Observer), which are expected to achieve precisions as low as 20-30 ppm (parts per million) [128, 129]. With the ability to measure transit depths as shallow as $\Delta F \sim 0.001\%$, these space transit surveys offer a promising avenue towards detecting the planetary systems that may have formed around CEMP stars.

The orbital period of a planet P , which can be determined if consecutive transits are observed, is given by Kepler’s third law in the case of a circular orbit,

$$P^2 = \frac{4\pi^2 a^3}{G(M_* + M_p)} \simeq \frac{4\pi^2 a^3}{GM_*} \quad (3.17)$$

where a is the orbital semi-major axis and the planetary mass is assumed to be negligible relative to the stellar mass, $M_p \ll M_*$, in the second equality. Given the relation we derived in equation (10) between the metallicity $[C/H]$ and the maximum semi-major axis allowed for a planet orbiting a CEMP star, the maximum orbital period of the planet can be expressed as a function of the metallicity of the host CEMP star ($M_* = 0.8 M_\odot$),

$$P_{\max} \simeq 365.25 \frac{10^{\frac{3}{2}([C/H] + \alpha)}}{\sqrt{M_*/M_\odot}} \text{ days} \quad (3.18)$$

where $\alpha \simeq 1.3, 1.7$, and 1.9 for carbon condensation efficiencies of 10%, 50%, and 100%. As can be seen in Figure 4, CEMP stars with higher carbon abundances $[C/H]$, i.e. G 77-61 and

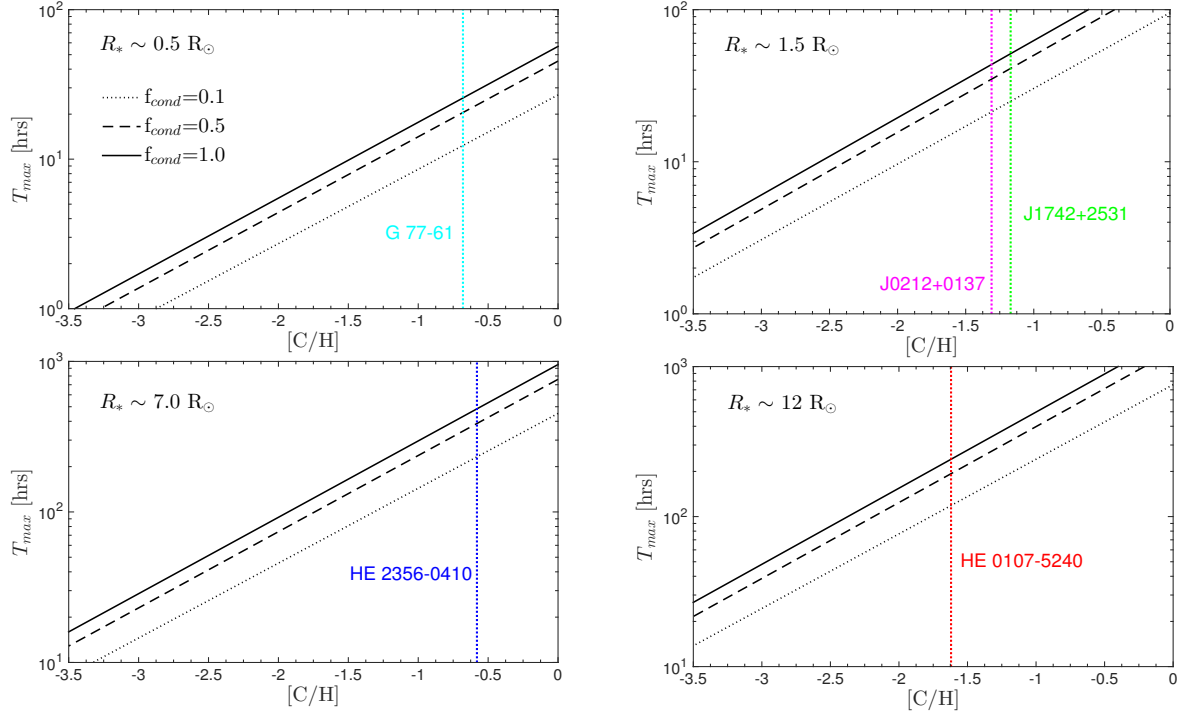


Figure 5. Maximum total transit duration of a carbon planet across its host CEMP star as a function of the star’s metallicity, expressed as the carbon abundance relative to that of the Sun, $[C/H]$. The dotted, dashed, and solid black curves denote the results obtained assuming carbon condensation efficiencies of 10%, 50%, and 100% in the parent CEMP star. The colored vertical lines represent the five CEMP stars considered here with measured carbon abundances $[C/H]$ and stellar radii derived using $R_* = \sqrt{GM_*/g}$ with mass $M_* = 0.8 M_\odot$.

HE 2356-0410, and larger efficiencies for carbon dust condensation f_{cond} , can host planets with wider orbits and slower rotations, resulting in transits as infrequently as once every couple hundred years. Conversely, carbon planets orbiting relatively less carbon-rich CEMP stars, like SDSS J0212+0137, are expected to have higher rates of transit reoccurrence, completing rotations around their parent stars every ~ 1 -10 years. These shorter period planets therefore have a much higher probability of producing an observable transit.

The maximum duration of the transit, T , can also be expressed as a function of the metallicity $[C/H]$ of the parent CEMP star. For transits across the center of a star, the total duration is given by,

$$T \simeq 2R_* \sqrt{\frac{a}{GM_*}} \quad (3.19)$$

with the assumption that $M_p \ll M_*$ and $R_p \ll R_*$. Once again, using the relation from equation (10) to express the maximum orbital distance from the host star in terms of the star’s carbon abundance, we find that the maximum transit duration of a carbon planet across its parent CEMP star ($M_* = 0.8 M_\odot$) is

$$T_{max} \simeq 13 \frac{R_*}{R_\odot} \sqrt{\frac{10^{[C/H]+\alpha}}{M_*/M_\odot}} \text{ hrs} . \quad (3.20)$$

In Figure 5, these maximum durations are shown as a function of $[C/H]$ for the various stellar radii associated with the CEMP stars we consider here. Transits across CEMP stars with larger radii and higher carbon abundances are expected to take much longer. While the total transit duration across SDSS J0212+0137 and SDSS J1742+2531 with $R_* \sim 1.5 R_\odot$ and metallicities of $[C/H] \sim -1.3 - -1.2$, is at most ~ 1 -2 days, transits across HE 0107-5240 ($R_* \sim 12 R_\odot$, $[C/H] \sim -1.6$) can take up to 2 weeks ($f_{cond} = 1$). In general, the geometric probability of a planet passing between the observer and the planet’s parent star increases with stellar radius and decreases with orbital radius, $p_t \simeq R_*/a$ [130]. Therefore, focusing on CEMP stars, such as HE 0107-5240 and HE 2356-0410, with large stellar radii increases the observer’s chance of spotting transits and detecting a planetary system.

3.6 Section Summary and Implications

We explored the possibility of carbon planet formation around the iron-deficient, carbon-rich subset of low-mass stars known as CEMP stars. The observed abundance patterns of CEMP-no stars suggest that these stellar objects were probably born out of gas enriched by massive first-generation stars that ended their lives as Type II SNe with low levels of mixing and a high degree of fallback. The formation of dust grains in the ejecta of these primordial core-collapsing SNe progenitors has been observationally confirmed and theoretically studied. In particular, amorphous carbon is the only grain species found to condense and form in non-negligible amounts in SN explosion models that are tailored to reproduce the abundance patterns measured in CEMP-no stars. Under such circumstances, the gas clouds which collapse and fragment to form CEMP-no stars and their protoplanetary disks may contain significant amounts of carbon dust grains imported from SNe ejecta. The enrichment of solid carbon in the protoplanetary disks of CEMP stars may then be further enhanced by Fischer-Tropsch-type reactions and carbon-rich condensation sequences, where the latter occurs specifically in nebular gas with $C/O \gtrsim 1$.

For a given metallicity $[C/H]$ of the host CEMP star, the maximum distance out to which planetesimal formation is possible can then be determined by comparing the dust-settling timescale in the protostellar disk to the expected disk lifetime. Assuming that disk dissipation is driven by a metallicity-dependent photoevaporation rate, we find a linear relation between $[C/H]$ and the maximum semi-major axis of a carbon planet orbiting its host CEMP star. Very carbon-rich CEMP stars, such as G 77-61 and HE 2356-0410 with $[C/H] \simeq -0.7 - -0.6$, can host carbon planets with semi-major axes as large ~ 20 AU for 100% carbon condensation efficiencies; this maximum orbital distance reduces to ~ 5 AU when the condensation efficiency drops by an order of magnitude. In the case of the observed CEMP-no stars HE 0107-5240, SDSS J0212+0137, and SDSS J1742+2531, where the carbon abundances are in the range $[C/H] \simeq -1.6 - -1.2$, we expect more compact orbits, with maximum orbital distances $r_{max} \simeq 2, 4$, and 6 AU, respectively, for $f_{cond} = 1$ and $r_{max} \simeq 0.5 - 1$ AU for $f_{cond} = 0.1$.

We then use the linear relation found between $[C/H]$ and r_{max} , along with the theoretical mass-radius relation derived for a solid, pure carbon planet (§4), to compute the three observable characteristics of planetary transits: the orbital period, the transit depth, and the transit duration. We find that the relative change in flux, ΔF , caused by an Earth-mass carbon planet transiting across its host CEMP star ranges from $\sim 0.0001\%$ for a stellar radius of $R_* \sim 10 R_\odot$ to $\sim 0.01\%$ for a solar-sized stellar host. While the shallow transit depths of Earth-mass carbon planets around HE 0107-5240 and HE 2356-0410 may evade detection, current and future space-based transit surveys promise to achieve the precision

levels ($\Delta F \sim 0.001\%$) necessary to detect planetary systems around CEMP stars such as SDSS J0212+0137, SDSS J1742+2531, and G 77-61. If gas giant (Jupiter scale) planets form around CEMP stars, their transits would be much easier to detect than rocky planets. However, they are not likely to host life as we know it.

Short orbital periods and long transit durations are also key ingredients in boosting the probability of transit detection by observers. G 77-61 is not an optimal candidate in these respects since given its large carbon abundance ($[C/Fe] \sim 3.4$), carbon planets may form out to very large distances and take up to a century to complete an orbit around the star for $f_{cond} = 1$ ($P_{max} \sim 10$ years for 10% carbon condensation efficiency). The small stellar radius, $R_* \sim 0.5 R_\odot$, also reduces chances of spotting the transit since the resulting transit duration is only ~ 30 hours at most. Carbon planets around larger CEMP stars with an equally carbon-rich protoplanetary disk, such as HE 2356-0410 ($R_* \sim 7 R_\odot$), have a better chance of being spotted, with transit durations lasting up to ~ 3 weeks. The CEMP-stars SDSS J0212+0137, and SDSS J1742+2531 are expected to host carbon planets with much shorter orbits, $P_{max} \sim 16$ years for 100% condensation efficiency ($P_{max} \sim 1$ year for $f_{cond} = 0.1$), and transit durations that last as long as ~ 60 hours. If the ability to measure transit depths improves to a precision of 1 ppm, then potential carbon planets around HE 0107-5240 are the most likely to be spotted (among the group of CEMP-no stars considered here), transiting across the host star at least once every ~ 5 months (10% condensation efficiency) with a transit duration of 6 days.

While our calculations place upper bounds on the distance from the host star out to which carbon planets can form, we note that orbital migration may alter a planet's location in the circumstellar disk. As implied by the existence of 'hot Jupiters', it is possible for a protoplanet that forms at radius r to migrate inward either through gravitational interactions with other protoplanets, resonant interactions with planetesimals with more compact orbits, or tidal interactions with gas in the surrounding disk [42]. Since Figure 3.3 only plots r_{max} , the *maximum* distance out to which a carbon planet with $[C/H]$ can form, our results remain consistent in the case of an inward migration. However, unless planets migrate inward from their place of birth in the disk, we do not expect to find carbon exoplanets orbiting closer than $r \simeq 0.02$ AU from the host stars since at such close proximities, temperatures are high enough to sublimate carbon dust grains.

Protoplanets can also be gravitationally scattered into wider orbits through interactions with planetesimals in the disk [131, 132]. Such an outward migration of carbon planets may result in observations that are inconsistent with the curves in Figure 3.3. A planet that formed at radius $r \ll r_{max}$ still has room to migrate outwards without violating the 'maximum distance' depicted in Figure 3.3; however, the outward migration of a carbon planet that originally formed at, or near, r_{max} would result in a breach of the upper bounds placed on the transiting properties of carbon planets (Section 5). In particular, a carbon planet that migrates to a semi-major axis $r > r_{max}$ will have an orbital period and a transit duration time that exceeds the limits prescribed in our equations.

Detection of the carbon planets that we suggest may have formed around CEMP stars will provide us with significant clues regarding how planet formation may have started in the early Universe. The formation of planetary systems not only signifies an increasing degree of complexity in the young Universe, but it also carries implications for the development of life at this early junction [3]. The lowest metallicity planetary system detected to date is around BD+20 24 57, a K2-giant with $[Fe/H] = -1.0$ [133], a metallicity already well below the critical value once believed to be necessary for planet formation [134, 135]. More recent

formulations of the minimum metallicity required for planet formation are consistent with this observation, estimating that the first Earth-like planets likely formed around stars with metallicities $[\text{Fe}/\text{H}] \lesssim -1.0$ [106]. The CEMP stars considered in this section are extremely iron-deficient, with $[\text{Fe}/\text{H}] \lesssim -3.2$, and yet, given the enhanced carbon abundances which dominate the total metal content in these stars ($[\text{C}/\text{H}] \gtrsim -1.6$), the formation of solid carbon exoplanets in the protoplanetary disks of CEMP stars remains a real possibility.

An observational program aimed at searching for carbon planets around these low-mass Population II stars could therefore potentially shed light on the question of how early planets, and subsequently, life could have formed after the Big Bang.

4 Water Formation During the Epoch of First Metal Enrichment

4.1 Section Background

Water is an essential ingredient for life as we know it [2]. In the interstellar medium (ISM) of the Milky-Way and also in external galaxies, water has been observed in the gas phase and as grain surface ice in a wide variety of environments. These environments include diffuse and dense molecular clouds, photon-dominated regions (PDRs), shocked gas, protostellar envelopes, and disks (see review by Ref. [136]).

In diffuse and translucent clouds, H_2O is formed mainly in gas phase reactions via ion-molecule sequences [137]. The ion-molecule reaction network is driven by cosmic-ray or X-ray ionization of H and H_2 , that leads to the formation of H^+ and H_3^+ ions. These interact with atomic oxygen and form OH^+ . A series of abstractions then lead to the formation of H_3O^+ , which makes OH and H_2O through dissociative recombination. This formation mechanism is generally not very efficient, and only a small fraction of the oxygen is converted into water, the rest remains in atomic form, or freezes out as water ice [138].

Ref. [139] showed that the abundance of water vapor within diffuse clouds in the Milky Way galaxy is remarkably constant, with $x_{\text{H}_2\text{O}} \sim 10^{-8}$, that is $\sim 0.1\%$ of the available oxygen. Here $x_{\text{H}_2\text{O}}$ is the H_2O number density relative to the total hydrogen nuclei number density. Towards the Galactic center this value can be enhanced by up to a factor of ~ 3 [140, 141].

At temperatures $\gtrsim 300$ K, H_2O may form directly via the neutral-neutral reactions, $\text{O} + \text{H}_2 \rightarrow \text{OH} + \text{H}$, followed by $\text{OH} + \text{H}_2 \rightarrow \text{H}_2\text{O} + \text{H}$. This formation route is particularly important in shocks, where the gas heats up to high temperatures, and can drive most of the oxygen into H_2O [142, 143].

Temperatures of a few hundreds K are also expected in very low metallicity gas environments, with elemental oxygen and carbon abundances of $\lesssim 10^{-3}$ solar [39, 144, 145], associated with the epochs of the first enrichment of the ISM with heavy elements, in the first generation of galaxies at high redshifts [5]. At such low metallicities, cooling by fine structure transitions of metal species such as the [CII] $158 \mu\text{m}$ line, and by rotational transitions of heavy molecules such as CO , becomes inefficient and the gas remains warm.

Could the enhanced rate of H_2O formation via the neutral-neutral sequence in such warm gas, compensate for the low oxygen abundance at low metallicities?

Ref. [144] studied the thermal and chemical evolution of collapsing gas clumps at low metallicities. They found that for models with gas metallicities of $10^{-3} - 10^{-4}$ solar, $x_{\text{H}_2\text{O}}$ may reach 10^{-8} , but only if the density, n , of the gas approaches 10^8 cm^{-3} . Photodissociation of molecules by far-ultraviolet (FUV) radiation was not included in their study. While at solar metallicity dust-grains shield the interior of gas clouds from the FUV radiation, at

low metallicities photodissociation by FUV becomes a major removal process for H_2O . H_2O photodissociation produces OH, which is then itself photodissociated into atomic oxygen.

Ref. [146] developed a theoretical model to study the abundances of various molecules, including H_2O , in PDRs. Their model included many important physical processes, such as freezeout of gas species, grain surface chemistry, and also photodissociation by FUV photons. However they focused on solar metallicity. Intriguingly, Ref. [147] report a water abundance close to 10^{-8} in the optically thick core of their single PDR model for a low metallicity of 10^{-2} (with $n = 10^3 \text{ cm}^{-3}$). However, Bayet et al. did not investigate the effects of temperature and UV intensity variations on the water abundance in the low metallicity regime.

Recently, a comprehensive study of molecular abundances for the bulk ISM gas as functions of the metallicity, were studied by Ref. [148] and Ref. [149]; these models however, focused on the “low temperature” ion-molecule formation chemistry.

In this section we present results for the H_2O abundance in low metallicity gas environments, for varying temperatures, FUV intensities and gas densities. We find that for temperatures T in the range $250 - 350 \text{ K}$, H_2O may be abundant, comparable to or higher than that found in diffuse Galactic clouds, provided that the FUV intensity to density ratio is smaller than a critical value.

4.2 Model Ingredients

We calculate the abundance of gas-phase H_2O for low metallicity gas parcels, that are exposed to external FUV radiation and cosmic-ray and/or X-ray fluxes. Given our chemical network we solve the steady state rate equations using our dedicated Newton-based solver, and obtain $x_{\text{H}_2\text{O}}$ as function of T and the FUV intensity to density ratio.

We adopt a 10^5 K diluted blackbody spectrum, representative of radiation produced by massive Pop-III stars. The photon density in the 6-13.6 eV interval, is $n_\gamma \equiv n_{\gamma,0} I_{\text{UV}}$, where $n_{\gamma,0} = 6.5 \times 10^{-3} \text{ photons cm}^{-3}$ is the photon density in the interstellar radiation field [ISRF, 150], and I_{UV} is the “normalized intensity”. Thus $I_{\text{UV}} = 1$ corresponds to the FUV intensity in the Draine ISRF.

Cosmic-ray and/or X-ray ionization drive the ion-molecule chemical network. We assume an ionization rate per hydrogen nucleon $\zeta \text{ (s}^{-1}\text{)}$. In the Galaxy, Ref. [151] and Ref. [152] showed that ζ lies within the relatively narrow range $10^{-15} - 10^{-16} \text{ s}^{-1}$. We therefore introduce the “normalized ionization rate” $\zeta_{-16} \equiv (\zeta/10^{-16} \text{ s}^{-1})$. The ionization rate and the FUV intensity are likely correlated, as both should scale with the formation rate of massive OB stars. We thus set $\zeta_{-16} = I_{\text{UV}}$ as our fiducial case but also consider the cases $\zeta_{-16} = 10^{-1} I_{\text{UV}}$ and $\zeta_{-16} = 10 I_{\text{UV}}$.

Dust shielding against the FUV radiation becomes ineffective at low metallicities. However, self absorption in the H_2 lines may significantly attenuate the destructive Lyman Werner (11.2-13.6 eV) radiation [153, 154] and high abundances of H_2 may be maintained even at low metallicity [149]. In the models presented here we assume an H_2 shielding column of at least $5 \times 10^{21} \text{ cm}^{-2}$. (For such conditions CO is also shielded by the H_2 .) The LW flux is then attenuated by a self-shielding factor of $f_{\text{shield}} \sim 10^{-8}$ and the H_2 photodissociation rate is only $5.8 \times 10^{-19} I_{\text{UV}} \text{ s}^{-1}$. With this assumption H_2 photodissociation by LW photons is negligible compared to cosmic-ray and/or X-ray ionization as long as $I_{\text{UV}} < 85 \zeta_{-16}$.

However, even when the Lyman Werner band is fully blocked, OH and H_2O are photodissociated because their energy thresholds for photodissociation are 6.4 and 6 eV, respectively. For the low metallicities that we consider, photodissociation is generally the dominant re-

moval mechanism for H₂O and OH. We adopt the calculated OH and H₂O photodissociation rates calculated by Ref. [149].

We assume thermal and chemical steady states. In the Milky Way, the bulk of the ISM gas is considered to be at approximate thermal equilibrium, set by cooling and heating processes. We discuss the relevant chemical and thermal time-scales in §4.4.

Given the above mentioned assumptions, the steady state solutions for the species abundances depend on only two parameters, the temperature T and the intensity to density ratio I_{UV}/n_4 . Here $n_4 \equiv (n/10^4 \text{ cm}^{-3})$ is the total number density of hydrogen nuclei normalized to typical molecular cloud densities. T and I_{UV}/n_4 form our basic parameter space in our study.

4.3 Chemical Model

We consider a chemical network of 503 two-body reactions, between 56 atomic, molecular and ionic species of H, He, C, O, S, and Si. We assume cosmological elemental helium abundance of 0.1 relative to hydrogen (by number). For the metal elemental abundances we adopt the photospheric solar abundances, multiplied by a metallicity factor Z' (i.e., $Z' = 1$ is solar metallicity). In our fiducial model we assume $Z' = 10^{-3}$, but we also explore cases with $Z' = 10^{-2}$ and $Z' = 10^{-4}$. Since our focus here is on the very low metallicity regime, where dust grains play a lesser role, we neglect any depletion on dust grains, and dust-grain chemistry (except for H₂, as discussed further below). Direct and induced ionizations and dissociations by the cosmic-ray / X-ray field ($\propto \zeta$) are included. For the gas phase reactions, we adopt the rate coefficients given by the UMIST 2012 database [155].

The formation of heavy molecules relies on molecular hydrogen. We consider two scenarios for H₂ formation: (a) pure gas-phase formation; and (b) gas-phase formation plus formation on dust grains. In gas-phase, radiative-attachment



followed by associative-detachment



is the dominant H₂ formation route.

H₂ formation on the surface of dust grains is considered to be the dominant formation channel in the Milky way. We adopt a standard rate coefficient [156–158],

$$R \simeq 3 \times 10^{-17} T_2^{1/2} Z' \text{ cm}^3 \text{ s}^{-1} \quad (4.3)$$

where $T_2 \equiv (T/100 \text{ K})$. In this expression we assume that the dust-to-gas ratio is linearly proportional to the metallicity Z' . Thus, in scenario (b) H₂ formation on dust grains dominates even for $Z' = 10^{-3}$. Scenario (a) is the limit where the gas-phase channel dominates, as appropriate for dust-free environments or for superlinear dependence of the dust-to-gas ratio on Z' .

4.4 Time scales

The timescale for the system to achieve chemical steady state is dictated by the relatively long H₂ formation timescale. In the gas phase (scenario [a]) it is

$$t_{\text{H}_2} = \frac{1}{k_2 n x_e} \approx 8 \times 10^8 \zeta_{-16}^{-1/2} n_4^{-1/2} T_2^{-1} \text{ yr} , \quad (4.4)$$

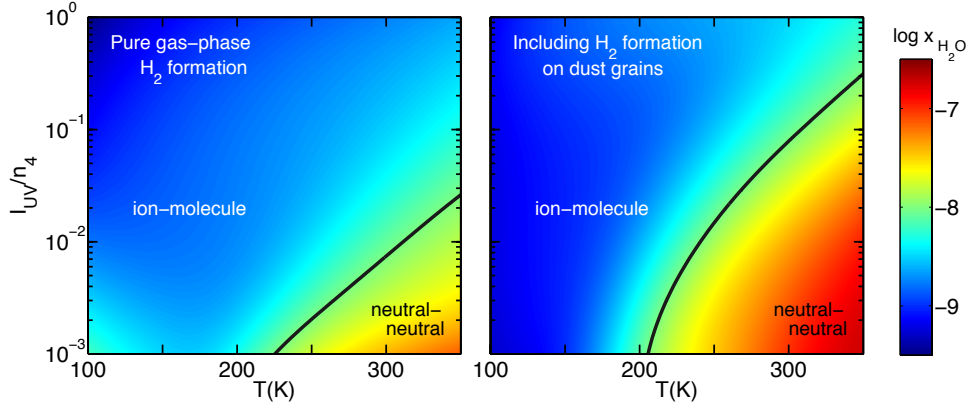


Figure 6. The fractional H_2O abundance $x_{\text{H}_2\text{O}}$ as a function of T and I_{UV}/n_4 , for $Z' = 10^{-3}$ and $\zeta_{-16}/I_{\text{UV}} = 1$, assuming pure gas-phase chemistry (scenario [a] - left panel), and including H_2 formation on dust grains (scenario [b] - right panels). In both panels, the solid line indicates the 10^{-8} contour, which is a characteristic value for the H_2O gas phase abundance in diffuse clouds within the Milky-Way galaxy. At high temperatures (or low I_{UV}/n_4 values) the neutral-neutral reactions become effective and $x_{\text{H}_2\text{O}}$ rises.

where $x_e = 2.4 \times 10^{-5} (\zeta_{-16}/n_4)^{1/2} T_2^{0.38}$ is the electron fraction as set by ionization recombination equilibrium, and $k_2 \approx 1.5 \times 10^{-16} T_2^{0.67} \text{ cm}^3 \text{ s}^{-1}$ is the rate coefficient for reaction (4.1).

For formation on dust grains ($\propto Z'$), the timescale is generally shorter, with

$$t_{\text{H}_2} = \frac{1}{Rn} \approx 10^8 T_2^{-1/2} n_4^{-1} \left(\frac{10^{-3}}{Z'} \right) \text{ yr} . \quad (4.5)$$

Gas clouds with lifetimes $t \gg t_{\text{H}_2}$ will reach chemical steady state.

The relevant timescale for thermal equilibrium is the cooling timescale. For low metallicity gas with $Z' = 10^{-3}$, the cooling proceeds mainly via H_2 rotational excitations [145]. If the cooling rate per H_2 molecule (in erg s^{-1}) is $W(n, T)$, then the cooling timescale is given by

$$t_{\text{cool}} = \frac{k_B T}{W(n, T)} . \quad (4.6)$$

Here k_B is the Boltzmann constant. For $n = 10^4 \text{ cm}^{-3}$, and $T = 300 \text{ K}$, $W \approx 5 \times 10^{-25} (x_{\text{H}_2}/0.1) \text{ erg s}^{-1}$ [159], and the cooling time is very short $\approx 2 \times 10^3 (0.1/x_{\text{H}_2}) \text{ yr}$. For densities much smaller than the critical density for H_2 cooling, $W \propto n$ and $t_{\text{cool}} \propto 1/n$. In the opposite limit, W saturates and t_{cool} becomes independent of density. We see that generally $t_{\text{cool}} \ll t_{\text{H}_2}$.

Because the free fall time

$$t_{\text{ff}} = \left(\frac{3\pi}{32G\rho} \right)^{1/2} = 5 \times 10^5 n_4^{-1/2} \text{ yr} , \quad (4.7)$$

is generally much shorter than t_{H_2} , chemical steady state may be achieved only in stable, non-collapsing clouds, with lifetimes $\gg t_{\text{ff}}$. Obviously both t_{H_2} and t_{cool} must be also shorter than the Hubble time at the redshift of interest.

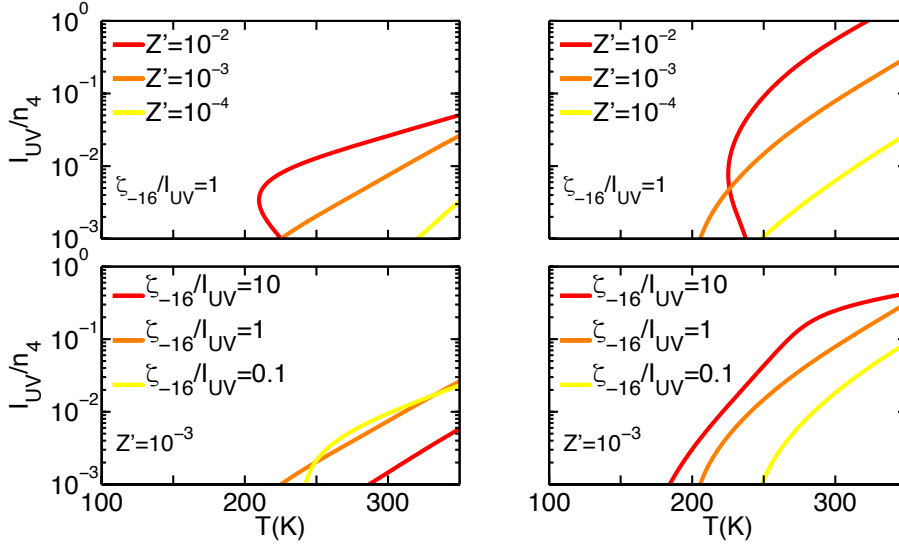


Figure 7. The $x_{\text{H}_2\text{O}} = 10^{-8}$ contour, for variations in Z' (upper panels) and in $\zeta_{-16}/I_{\text{UV}}$ (lower panels), assuming pure gas-phase chemistry (scenario [a] - left panels), and including H_2 formation on dust grains (scenario [b] - right panels).

4.5 Results

Next we present and discuss our results for the steady state, gas-phase H_2O fraction $x_{\text{H}_2\text{O}} \equiv n_{\text{H}_2\text{O}}/n$, as function of temperature T , and the FUV intensity to density ratio I_{UV}/n_4 .

4.6 $x_{\text{H}_2\text{O}}$ as a function of T and I_{UV}/n_4

Figure 6 shows $\log_{10}(x_{\text{H}_2\text{O}})$ contours for the two scenarios described in § 4.3. In one H_2 forms in pure gas-phase (scenario [a] - left panel), and in the other H_2 forms also on dust-grains (scenario [b] - right panel). Our fiducial parameters are $Z' = 10^{-3}$ and $\zeta_{-16} = I_{\text{UV}}$. At the upper-left region of the parameter space, $x_{\text{H}_2\text{O}}$ is generally low $\lesssim 10^{-9}$. In this regime, H_2O forms through the ion-molecule sequence, that is operative at low temperatures. In the lower right corner, the neutral-neutral reactions become effective and $x_{\text{H}_2\text{O}}$ rises.

In both panels, the solid line highlights the $x_{\text{H}_2\text{O}} = 10^{-8}$ contour, which resembles the H_2O gas phase abundance in diffuse and translucent Milky Way clouds. This line also delineates the borderline between the regimes where H_2O forms via the “cold” ion-molecule sequence, and the “warm” neutral-neutral sequence. The temperature range at which the neutral-neutral sequence kicks-in is relatively narrow $\sim 250 - 350$ K, because the neutral-neutral reactions are limited by energy barriers that introduce an exponential dependence on temperature.

The dependence on I_{UV}/n_4 is introduced because the FUV photons photodissociate OH and H_2O molecules and therefore increase the removal rate of H_2O and at the same time suppress formation via the $\text{OH} + \text{H}_2$ reaction. This gives rise to a critical value for I_{UV}/n_4 below which H_2O may become abundant.

For pure gas-phase H_2 formation (scenario [a] - left panel), the gas remains predominantly atomic, and H_2O formation is less efficient. In this case $x_{\text{H}_2\text{O}} \gtrsim 10^{-8}$ only when I_{UV}/n_4 is smaller than a critical value of

$$(I_{\text{UV}}/n_4)_{\text{crit}}^{(a)} = 2 \times 10^{-2} \quad . \quad (4.8)$$

However, when H_2 formation on dust is included (scenario [b] - right panel), the hydrogen becomes fully molecular, and H_2O formation is then more efficient. In this case $x_{\text{H}_2\text{O}}$ may reach 10^{-8} for I_{UV}/n_4 smaller than

$$(I_{\text{UV}}/n_4)_{\text{crit}}^{(\text{b})} = 3 \times 10^{-1} \quad , \quad (4.9)$$

an order of magnitude larger than for the pure-gas phase formation scenario.

4.7 Variations in Z' and $\zeta_{-16}/I_{\text{UV}}$

In Figure 7 we investigate the effects of variations in the value of Z' and the normalization $\zeta_{-16}/I_{\text{UV}}$. The Figure shows the $x_{\text{H}_2\text{O}} = 10^{-8}$ contours for scenarios (a) (left panels) and (b) (right panels). As discussed above, H_2O is generally more abundant in scenario (b) because the hydrogen is fully molecular in this case, and therefore the 10^{-8} contours are located at higher I_{UV}/n_4 values in both right panels.

The upper panels show the effect of variations in the metallicity value Z' , for our fiducial normalization $\zeta_{-16} = I_{\text{UV}}$. In both panels, the oxygen abundance rises, and $x_{\text{H}_2\text{O}}$ increases with increasing Z' . Thus at higher Z' , the 10^{-8} contours shift to lower T and higher I_{UV}/n_4 and vice versa. An exception is the behavior of the $Z' = 10^{-2}$ curve, for which the metallicity is already high enough so that reactions with metal species dominate H_2O removal for $I_{\text{UV}}/n_4 \lesssim 10^{-2}$. The increase in metallicity then results in a *decrease* of the H_2O abundance, and the 10^{-8} contour shifts to the right. For $I_{\text{UV}}/n_4 \gtrsim 10^{-2}$ removal by FUV dominates and the behavior is similar to that in the $Z' = 10^{-3}$ and $Z' = 10^{-4}$ cases.

The lower panels show the effects of variations in the ionization rate normalization $\zeta_{-16}/I_{\text{UV}}$ for our fiducial metallicity value of $Z' = 10^{-3}$. First we consider the pure gas phase formation case (scenario [a] - lower left panel). For the two cases $\zeta_{-16}/I_{\text{UV}} = 1$ and 10^{-1} , the H_2O removal is dominated by FUV photodissociation and therefore is independent of ζ . As shown by Ref. [149], the H_2O formation rate is also independent of ζ when the H_2 forms in the gas-phase. Therefore $x_{\text{H}_2\text{O}}$ is essentially independent of ζ and the contours overlap. For the high ionization rate $\zeta_{-16}/I_{\text{UV}} = 10$, the proton abundance becomes high, and H_2O reactions with H^+ dominate H_2O removal. In this limit $x_{\text{H}_2\text{O}}$ decreases with ζ and the 10^{-8} contour moves down.

When H_2 forms on dust (scenario [b] - lower right panel), the H_2O formation rate via the ion-molecule sequence is proportional to the H^+ and H_3^+ abundances, which rise with ζ . Since the gas is molecular, the proton fraction is low and the removal is always dominated by FUV photodissociations (independent of ζ). Therefore, in this case $x_{\text{H}_2\text{O}}$ *increases* with $\zeta_{-16}/I_{\text{UV}}$ and the curves shift up and to the left, toward lower T and higher I_{UV}/n_4 .

4.8 Section Summary and Implications

We have demonstrated that the H_2O gas phase abundance may remain high even at very low metallicities of $Z' \sim 10^{-3}$. The onset of the efficient neutral-neutral formation sequence at $T \sim 300$ K, may compensate for the low metallicity, and form H_2O in abundance similar to that found in diffuse clouds within the Milky Way.

We have considered two scenarios for H_2 formation, representing two limiting cases, one in which H_2 is formed in pure gas phase (scenario [a]), and one in which H_2 forms both in gas-phase and on dust grains, assuming that the dust abundance scales linearly with Z' (scenario [b]). Recent studies by Refs. [160–162] suggest that the dust abundance might decrease faster than linearly with decreasing Z' . As shown by Ref. [149], for $Z' = 10^{-3}$ and

dust abundance that scales as Z'^β with $\beta \geq 2$, H_2 formation is dominated by the gas phase formation channel. Therefore our scenario (a) is also applicable for models in which dust grains are present, with an abundance that scales superlinearly with Z' . For both scenarios (a) and (b) we have found that the neutral-neutral formation channel yields $x_{\text{H}_2\text{O}} \gtrsim 10^{-8}$, provided that I_{UV}/n_4 is smaller than a critical value. For the first scenario we have found that this critical value is $(I_{\text{UV}}/n_4)_{\text{crit}} = 2 \times 10^2$. For the second scenario $(I_{\text{UV}}/n_4)_{\text{crit}} = 3 \times 10^{-1}$.

In our analysis we have assumed that the system had reached a chemical steady state. For initially atomic (or ionized) gas, this assumption offers the best conditions for the formation of molecules. However, chemical steady state might not always be achieved within a cloud lifetime or even within the Hubble time. The timescale to achieve chemical steady state (from an initially dissociated state) is dictated by the H_2 formation process, and is generally long at low metallicities. For $Z' = 10^{-3}$ and our fiducial parameters, the timescales for both scenarios are of order of a few 10^8 years (see e.g. Ref. [163]), and are comparable to the age of the Universe at redshifts of ~ 10 . The generically high water abundances we find for warm conditions and low metallicities will be maintained in dynamically evolving systems so long as they remain H_2 -shielded.

Our results might have interesting implications for the question of how early could have life originated in the Universe [3]. Our study addresses the first step of H_2O formation in early enriched, molecular gas clouds. If such a cloud is to collapse and form a protoplanetary disk, some of the H_2O may make its way to the surfaces of forming planets [136]. However, the question of to what extent the H_2O molecules that were formed in the initial molecular clouds, are preserved all the way through the process of planet formation, is beyond the scope of this section.

5 An Observational Test for the Anthropic Origin of the Cosmological Constant

5.1 Section Background

The distance to Type Ia supernovae [164, 165] and the statistics of the cosmic microwave background anisotropies [18] provide conclusive evidence for a finite vacuum energy density of $\rho_V = 4 \text{ keV cm}^{-3}$ in the present-day Universe. This value is a few times larger than the mean cosmic density of matter today. The expected exponential expansion of the Universe in the future (for a time-independent vacuum density) will halt the growth of all bound systems such as galaxies and groups of galaxies [166–168]. It will also redshift all extragalactic sources out of detectability (except for the merger remnant of the Milky Way and the Andromeda galaxies to which we are bound) – marking the end of extragalactic astronomy, as soon as the Universe will age by another factor of ten [169].

The observed vacuum density is smaller by tens of orders of magnitude than any plausible zero-point scale of the Standard Model of particle physics. Weinberg [34] first suggested that such a situation could arise in a theory that allows the cosmological constant to be a free parameter. On a scale much bigger than the observable Universe one could then find regions in which the value of ρ_V is very different. However, if one selects those regions that give life to observers, then one would find a rather limited range of ρ_V values near its observed magnitude, since observers are most likely to appear in galaxies as massive as the Milky-way galaxy which assembled at the last moment before the cosmological constant started to dominate our Universe. Vilenkin [170] showed that this so-called “anthropic argument” [171] can be used to calculate the probability distribution of vacuum densities with

testable predictions. This notion [23, 36, 172–175] gained popularity when it was realized that string theory predicts the existence of an extremely large number [176–179], perhaps as large as $\sim 10^{100}$ to 10^{500} [180], of possible vacuum states. The resulting landscape of string vacua [181] in the “multiverse” encompassing a volume of space far greater than our own inflationary patch, made the anthropic argument appealing to particle physicists and cosmologists alike [36, 182, 183].

The time is therefore ripe to examine the prospects for an experimental test of the anthropic argument. Any such test should be welcomed by proponents of the anthropic argument, since it would elevate the idea to the status of a falsifiable physical theory. At the same time, the test should also be welcomed by opponents of anthropic reasoning, since such a test would provide an opportunity to diminish the predictive power of the anthropic proposal and suppress discussions about it in the scientific literature.

Is it possible to dispute the anthropic argument without visiting regions of space that extend far beyond the inflationary patch of our observable Universe? The answer is *yes* if one can demonstrate that life could have emerged in our Universe even if the cosmological constant would have had values that are much larger than observed. In this section we propose a set of astronomical observations that could critically examine this issue. We make use of the fact that dwarf galaxies formed in our Universe at redshifts as high as $z \sim 10$ when the mean matter density was larger by a factor of $\sim 10^3$ than it is today⁵ [5]. If habitable planets emerged within these dwarf galaxies or their descendents (such as old globular clusters which might be the tidally truncated relics of early galaxies [184, 185]), then life would have been possible in a Universe with a value of ρ_V that is a thousand times bigger than observed.

5.2 Prior Probability Distribution of Vacuum Densities

On the Planck scale of a quantum field theory which is unified with gravity (such as string theory), the vacuum energy densities under discussion represent extremely small deviations around $\rho_V = 0$. Assuming that the prior probability distribution of vacuum densities, $\mathcal{P}_*(\rho_V)$, is not divergent at $\rho_V = 0$ (since $\rho_V = 0$ is not favored by any existing theory), it is natural to expand it in a Taylor series and keep only the leading term. Thus, in our range of interest of ρ_V values [174, 175],

$$\mathcal{P}_*(\rho_V) \approx \text{const.} \quad (5.1)$$

This implies that the probability of measuring a value equal to or smaller than the observed value of ρ_V is $\sim 10^{-3}$ if habitable planets could have formed in a Universe with a value of ρ_V that is a thousand times bigger than observed.

Numerical simulations indicate that our Universe would cease to make new bound systems in the near future [166–168]. A Universe in which ρ_V is a thousand times larger, would therefore make dwarf galaxies until $z \sim 10$ when the matter density was a thousand times larger than today. The question of whether planets can form within these dwarf galaxies can be examined observationally as we discuss next. It is important to note that once a dwarf galaxy forms, it has an arbitrarily long time to convert its gas into stars and planets, since its internal evolution is decoupled from the global expansion of the Universe (as long as outflows do not carry material out of its gravitational pull).

⁵We note that although the cosmological constant started to dominate the mass density of our Universe at $z \sim 0.4$, its impact on the formation of bound objects became noticeable only at $z \sim 0$ or later [166–168]. For the purposes of our discussion, we therefore compare the matter density at $z \sim 10$ to that today. Coincidentally, the Milky-Way galaxy formed before ρ_V dominated but it could have also formed later.

5.3 Extragalactic Planet Searches

Gravitational microlensing is the most effective search method for planets beyond our galaxy. The planet introduces a short-term distortion to the otherwise smooth lightcurve produced by its parent star as that star focuses the light from a background star which happens to lie behind it [186]–[187]. In an extensive search for planetary microlensing signatures, a number of collaborations named PLANET [188], μ FUN [189] and RoboNET, are performing follow-up observations on microlensing events which are routinely detected by the groups MOA [190] and OGLE [191]. Many “planetary” events have been reported, including a planet of a mass of ~ 5 Earth masses at a projected separation of 2.6AU from a $0.2M_{\odot}$ M-dwarf star in the microlensing event OGLE-2005-BLG-390Lb [192], and a planet of 13 Earth masses at a projected separation of 2.3AU from its parent star in the event OGLE-2005-BLG-169 towards the Galactic bulge – in which the background star was magnified by the unusually high factor of ~ 800 [193]. Based on the statistics of these events and the search parameters, one can infer strong conclusions about the abundance of planets of various masses and orbital separations in the surveyed star population [193–195]. The technique can be easily extended to lenses outside our galaxy and out to the Andromeda galaxy (M31) using the method of pixel lensing [196–198]. For the anthropic experiment, we are particularly interested in applying this search technique to lensing of background Milky-Way stars by old stars in foreground globular clusters (which may be the tidally-truncated relics of $z \sim 10$ galaxies), or to lensing of background M31 stars by foreground globular clusters [199] or dwarf galaxies such as Andromeda VIII [200]. In addition, self-lensing events in which foreground stars of a dwarf galaxy lens background stars of the same galaxy, are of particular interest. Such self-lensing events were observed in the form of caustic-crossing binary lens events in the Large Magellanic Cloud (LMC) and the Small Magellanic Cloud (SMC) [201]. In the observed cases there is enough information to ascertain that the most likely lens location is in the Magellanic Clouds themselves. Yet, each caustic-crossing event represents a much larger number of binary lens events from the same lens population; the majority of these may be indistinguishable from point-lens events. It is therefore possible that some of the known single-star LMC lensing events are due to self-lensing [201], as hinted by their geometric distribution [202, 203].

Another method for finding extra-Galactic planets involves transit events in which the planet passes in front of its parent star and causes a slight temporary dimming of the star. Spectral modeling of the parent star allows to constrain both the size and abundance statistics of the transiting planets [204, 205]. Existing surveys reach distance scales of several kpc [206]–[207] with some successful detections [208–210]. So far, a Hubble Space Telescope search for transiting Jupiters in the globular cluster 47 Tucanae resulted in no detections [211] [although a pulsar planet was discovered later by a different technique in the low-metallicity globular cluster Messier 4 [212], potentially indicating early planet formation]. A future space telescope (beyond the previous Kepler ⁶ and COROT ⁷ missions which focus on nearby stars) or a large-aperture ground-based facility (such as the Giant Magellan Telescope [GMT]⁸, the Thirty-Meter Telescope [TMT]⁹, or the European Extremely Large Telescope [EELT]¹⁰) could extend the transit search technique to planets at yet larger distances (but see Ref. [205]). Ex-

⁶<http://kepler.nasa.gov/>

⁷<http://smc.cnes.fr/COROT/>

⁸<http://www.gmto.org/>

⁹<http://www.tmt.org/>

¹⁰<http://www.eso.org/sci/facilities/eelt>

isting searches [204] identified the need for a high signal-to-noise spectroscopy as a follow-up technique for confirming real transits out of many false events. Such follow-ups would become more challenging at large distances, making the microlensing technique more practical.

5.4 Observations of Dwarf Galaxies at High-redshifts

Our goal is to study stellar systems in the local Universe which are the likely descendents of the early population of $z \sim 10$ galaxies [213]. In order to refine this selection, it would be desirable to measure the characteristic size, mass, metallicity, and star formation histories of $z \sim 10$ galaxies (see Ref. [5] for a review on their theoretically-expected properties). As already mentioned, it is possible that the oldest globular clusters are descendents of the first galaxies [214].

Recently, a large number of faint early galaxies, born less than a billion years after the big bang, have been discovered (see, e.g. [215, 216]). These include starburst galaxies with star formation rates in excess of $\sim 0.1 M_{\odot} \text{ yr}^{-1}$ and dark matter halos [217] of $\sim 10^{9-11} M_{\odot}$ [215, 218–221] at $z \sim 5-10$. Luminous Ly α emitters are routinely identified through continuum dropout and narrow band imaging techniques [220, 221]. In order to study fainter sources which were potentially responsible for reionization, spectroscopic searches have been undertaken near the critical curves of lensing galaxy clusters [216, 219], where gravitational magnification enhances the flux sensitivity. Because of the foreground emission and opacity of the Earth’s atmosphere, it is difficult to measure spectral features other than the Ly α emission line from these feeble galaxies from ground-based telescopes.

In one example, gravitational lensing by the massive galaxy cluster A2218 allowed to detect a stellar system at $z = 5.6$ with an estimated mass of $\sim 10^6 M_{\odot}$ in stars [219]. Detection of additional low mass systems could potentially reveal whether globular clusters formed at these high redshifts. Such a detection would be feasible with the *James Webb Space Telescope*¹¹. Existing designs for future large-aperture ($> 20\text{m}$) infrared telescopes (such as the GMT, TMT, and EELT mentioned above), would also enable to measure the spectra of galaxies at $z \sim 10$ and infer their properties.

Based the characteristics of high- z galaxies, one would be able to identify present-day systems (such as dwarf galaxies or globular clusters) that are their likely descendents [222, 223] and search for planets within them. Since the lifetime of massive stars that explode as core-collapse supernovae is two orders of magnitude shorter than the age of the universe at $z \sim 10$, it is possible that some of these systems would be enriched to a high metallicity despite their old age. For example, the cores of quasar host galaxies are known to possess super-solar metallicities at $z \gtrsim 6$ [224].

5.5 Section Summary and Implications

In future decades it would be technologically feasible to search for microlensing or transit events in local dwarf galaxies or old globular clusters and to check whether planets exist in these environments. Complementary observations of early dwarf galaxies at redshifts $z \sim 10$ can be used to identify nearby galaxies or globular clusters that are their likely descendents. If planets are found in local galaxies that resemble their counterparts at $z \sim 10$, then the precise version of the anthropic argument [34, 170, 172, 173, 175] would be weakened considerably, since planets could have formed in our Universe even if the cosmological constant, ρ_V , was three orders of magnitude larger. For a flat probability distribution at these ρ_V values (which

¹¹<http://www.jwst.nasa.gov/>

represents infinitesimal deviations from $\rho_V = 0$ relative to the Planck scale), this would imply that the probability for us to reside in a region where ρ_V obtains its observed value is lower than $\sim 10^{-3}$. The precise version of the anthropic argument [34, 170, 172, 173, 175] could then be ruled-out at a confidence level of $\sim 99.9\%$, which is a satisfactory measure for an experimental test. The envisioned experiment resonates with two of the most active frontiers in astrophysics, namely the search for planets and the study of high-redshift galaxies, and if performed it would have many side benefits to conventional astrophysics.

We note that in the hypothetical Universe with a large cosmological constant, life need not form at $z \sim 10$ (merely 400 million years after the big bang) but rather any time later. Billions of years after a dwarf galaxy had formed – a typical astronomer within it would see the host galaxy surrounded by a void which is dominated by the cosmological constant.

An additional factor that enters the likelihood function of ρ_V values involves the conversion efficiency of baryons into observers in the Universe. A Universe in which observers only reside in galaxies that were made at $z \sim 10$ might be less effective at making observers. The fraction of baryons that have assembled into star-forming galaxies above the hydrogen cooling threshold by $z \sim 10$ is estimated to be $\sim 10\%$ [5], comparable to the final fraction of baryons that condensed into stars in the present-day Universe [225]. It is possible that more stars formed in smaller systems down to the Jeans mass of $\sim 10^{4-5} M_\odot$ through molecular hydrogen cooling [15]. Although today most baryons reside in a warm-hot medium of $\sim 2 \times 10^6 \text{K}$ that cannot condense into stars [226, 227], most of the cosmic gas at $z \sim 10$ was sufficiently cold to fragment into stars as long as it could have cooled below the virial temperature of its host halos [5]. The star formation efficiency can be inferred [222] from dynamical measurements of the star and dark matter masses in local dwarfs or globulars that resemble their counterparts at $z \sim 10$. If only a small portion of the cosmic baryon fraction (Ω_b/Ω_m) in dwarf galaxies is converted into stars, then the probability of obtaining habitable planets would be reduced accordingly. Other physical factors, such as metallicity, may also play an important role. Preliminary evidence indicates that planet formation favors environments which are abundant in heavy elements [228], although notable exceptions exist [212].

Unfortunately, it is not possible to infer the planet production efficiency for an alternative Universe purely based on observations of our Universe. In our Universe, most of the baryons which were assembled into galaxies by $z \sim 10$ are later incorporated into bigger galaxies. The vast majority of the $z \sim 10$ galaxies are consumed through hierarchical mergers to make bigger galaxies; isolated descendants of $z \sim 10$ galaxies are rare among low-redshift galaxies. At any given redshift below 10, it would be difficult to separate observationally the level of planet formation in our Universe from the level that would have occurred otherwise in smaller galaxies if these were not consumed by bigger galaxies within a Universe with a large vacuum density, ρ_V . In order to figure out the planet production efficiency for a large ρ_V , one must adopt a strategy that mixes observations with theory. Suppose we observe today the planet production efficiency in the descendants of $z \sim 10$ galaxies. One could then use numerical simulations to calculate the abundance that these galaxies would have had today if ρ_V was $\sim 10^3$ times bigger than its observed value. This approach takes implicitly into account the possibility that planets may form relatively late (after ~ 10 Gyr) within these isolated descendants, irrespective of the value of ρ_V . The late time properties of gravitationally-bound systems are expected to be independent of the value of ρ_V .

In our discussion, we assumed that as long as rocky planets can form at orbital radii that allow liquid water to exist on their surface (the so-called *habitable zone* [2]), life would develop over billions of years and eventually mature in intelligence. Without a better understanding

of the origin of intelligent life, it is difficult to assess the physical conditions that are required for intelligence to emerge beyond the minimal requirements stated above. If life forms early then civilizations might have more time to evolve to advanced levels. On the other hand, life may be disrupted more easily in early galaxies because of their higher density (making the likelihood of stellar encounters higher) [36, 175], and so it would be useful to determine the environmental density observationally. In the more distant future, it might be possible to supplement the study proposed here by the more adventurous search for radio signals from intelligent civilizations beyond the boundaries of our galaxy. Such a search would bring an extra benefit. If the anthropic argument turns out to be wrong and intelligent civilizations are common in nearby dwarf galaxies, then the older more advanced civilizations among them might broadcast an explanation for why the cosmological constant has its observed value.

6 The Relative Likelihood of Life as a Function of Cosmic Time

6.1 Section Background

Currently, we only know of life on Earth. The Sun formed ~ 4.6 Gyr ago and has a lifetime comparable to the current age of the Universe. But the lowest mass stars near the hydrogen burning threshold at $0.08M_{\odot}$ could live a thousand times longer, up to 10 trillion years [229, 230]. Given that habitable planets may have existed in the distant past and might exist in the distant future, it is natural to ask: *what is the relative probability for the emergence of life as a function of cosmic time?* In this section, we answer this question conservatively by restricting our attention to the context of “life as we know it” and the standard cosmological model (Λ CDM).¹² Note that since the probability distribution is normalized to have a unit integral, it only compares the relative importance of different epochs for the emergence of life but does not calibrate the overall likelihood for life in the Universe. This feature makes our results robust to uncertainties in normalization constants associated with the likelihood for life on habitable planets.

Next we express the relative likelihood for the appearance of life as a function of cosmic time in terms of the star formation history of the Universe, the stellar mass function, the lifetime of stars as a function of their mass, and the probability of Earth-mass planets in the habitable zone of these stars. We define this likelihood within a fixed comoving volume which contains a fixed number of baryons. In predicting the future, we rely on an extrapolation of star formation rate until the current gas reservoir of galaxies is depleted.

6.2 Formalism

6.2.1 Master Equation

We wish to calculate the probability $dP(t)/dt$ for life to form on habitable planets per unit time within a fixed comoving volume of the Universe. This probability distribution should span the time interval between the formation time of the first stars (~ 30 Myr after the Big Bang) and the maximum lifetime of all stars that were ever made (~ 10 Tyr).

¹²We address this question from the perspective of an observer in a single comoving Hubble volume formed after the end of inflation. As such we do not consider issues of self-location in the multiverse, nor of the measure on eternally inflating regions of space-time. We note, however, that any observers in a post-inflationary bubble will by necessity of the eternal inflationary process, only be able to determine the age of their own bubble. We therefore restrict our attention to the question of the probability distribution of life in the history of our own inflationary bubble.

The probability $dP(t)/dt$ involves a convolution of the star formation rate per comoving volume, $\dot{\rho}_*(t')$, with the temporal window function, $g(t - t', m)$, due to the finite lifetime of stars of different masses, m , and the likelihood, $\eta_{\text{Earth}}(m)$, of forming an Earth-mass rocky planet in the habitable zone (HZ) of stars of different masses, given the mass distribution of stars, $\xi(m)$, times the probability, $p(\text{life}|\text{HZ})$, of actually having life on a habitable planet. With all these ingredients, the relative probability per unit time for life within a fixed comoving volume can be written in terms of the double integral,

$$\frac{dP}{dt}(t) = \frac{1}{N} \int_0^t dt' \int_{m_{\min}}^{m_{\max}} dm' \xi(m') \dot{\rho}_*(t', m') \eta_{\text{Earth}}(m') p(\text{life}|\text{HZ}) g(t - t', m'), \quad (6.1)$$

where the pre-factor $1/N$ assures that the probability distribution is normalized to a unit integral over all times. The window function, $g(t - t', m)$, determines whether a habitable planet that formed at time t' is still within a habitable zone at time t . This function is non-zero within the lifetime $\tau_*(m)$ of each star, namely $g(t - t', m) = 1$ if $0 < (t - t') < \tau_*(m)$, and zero otherwise. The quantities m_{\min} and m_{\max} represent the minimum and maximum masses of viable host stars for habitable planets, respectively. Below we provide more details on each of the various components of the above master equation.

6.2.2 Stellar Mass Range

Life requires the existence of liquid water on the surface of Earth-mass planets during the main stage lifetime of their host star. These requirements place a lower bound on the lifetime of the host star and thus an upper bound on its mass.

There are several proxies for the minimum time needed for life to emerge. Certainly the star must live long enough for the planet to form, a process which took ~ 40 Myr for Earth [231]. Moreover, once the planet formed, sufficient cooling must follow to allow the condensation of water on the planet's surface. The recent discovery of the earliest crystals, Zircons, suggest that these were formed during the Archean era, as much as 160 Myr after the planet formed [232]. Thus, we arrive at a conservative minimum of 200 Myr before life could form - any star living less than this time could not host life on an Earth-like planet. At the other end of the scale, we find that the earliest evidence for life on Earth comes from around 800 Myr after the formation of the planet [231], yielding an upper bound on the minimum lifetime of the host star. For the relevant mass range of massive stars, the lifetime, τ_* , scales with stellar mass, m , roughly as $(\tau_*/\tau_{\odot}) = (m/M_{\odot})^{-3}$, where $\tau_{\odot} \approx 10^{10}$ yr. Thus, we find that the maximum mass of a star capable of hosting life (m_{\max}) is in the range $2.3\text{--}3.7M_{\odot}$. Due to their short lifetimes and low abundances, high mass stars do not provide a significant contribution to the probability distribution, $dP(t)/dt$, and so the exact choice of the upper mass cutoff in the above range is unimportant. The lowest mass stars above the hydrogen burning threshold have a mass $m = 0.08M_{\odot}$.

6.2.3 Time Range

The first stars are predicted to have formed at a redshift of $z \sim 70$, about 30 Myr after the Big Bang [3, 5–7]. Their supernovae resulted in a second generation of stars – enriched by heavy elements, merely a few Myr later. The theoretical expectation that the second generation stars should have hosted planetary systems can be tested observationally by searching for planets around metal poor stars in the halo of the Milky Way galaxy [8].

Star formation is expected to exhaust the cold gas in galaxies as soon as the Universe will age by a factor of a few (based on the ratio between the current reservoir of cold gas in galaxies [225] and the current star formation rate), but low mass stars would survive long after that. The lowest mass stars near the hydrogen burning limit of $0.08M_{\odot}$, have a lifetime of order 10 trillion years [229]. The probability $dP(t)/dt$ is expected to vanish beyond that time.

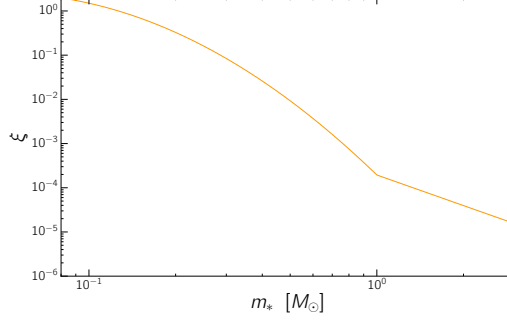


Figure 8. The Chabrier [233] mass function of stars, $\xi(m_*)$, plotted with a normalization integral of unity.

6.2.4 Initial Mass Function

The initial mass function (IMF) of stars $\xi(m)$ is proportional to the probability that a star in the mass range between m and $m + dm$ is formed. We adopt the empirically-calibrated, Chabrier functional form [233], which follows a lognormal form for masses under a solar mass, and a power law above a solar mass, as follows:

$$\xi(m) \propto \begin{cases} \left(\frac{m}{M_{\odot}}\right)^{-2.3} & m > 1 M_{\odot} \\ a \exp\left(-\frac{\ln(m/m_c)^2}{2\sigma^2}\right) \frac{M_{\odot}}{m} & m \leq 1 M_{\odot} \end{cases}, \quad (6.2)$$

where $a = 790$, $\sigma = 0.69$, and $m_c = 0.08M_{\odot}$. This IMF is plotted as a probability distribution normalized to a unit integral in Figure 8.

For simplicity, we ignore the evolution of the IMF with cosmic time and its dependence on galactic environment (e.g., galaxy type or metallicity [234]), as well as the uncertain dependence of the likelihood for habitable planets around these stars on metallicity [8].

6.2.5 Stellar Lifetime

The lifetime of stars, τ_* , as a function of their mass, m , can be modelled through a piecewise power-law form. For $m < 0.25M_{\odot}$, we follow Ref. [229]. For $0.75M_{\odot} < m < 3M_{\odot}$, we adopt a scaling with an average power law index of -2.5 and the proper normalization for the Sun [235]. Finally, we interpolate in the range between 0.25 and 0.75 M_{\odot} by fitting a

power-law form there and enforcing continuity. In summary, we adopt,

$$\tau_*(m) = \begin{cases} 1.0 \times 10^{10} \text{ yr} \left(\frac{m}{M_\odot} \right)^{-2.5} & 0.75M_\odot < m < 3M_\odot \\ 7.6 \times 10^9 \text{ yr} \left(\frac{m}{M_\odot} \right)^{-3.5} & 0.25M_\odot < m \leq 0.75M_\odot \\ 5.3 \times 10^{10} \text{ yr} \left(\frac{m}{M_\odot} \right)^{-2.1} & 0.08M_\odot \leq m \leq 0.25M_\odot \end{cases}. \quad (6.3)$$

This dependence is depicted in Figure 9.

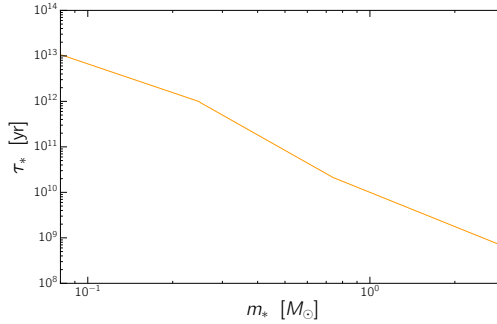


Figure 9. Stellar lifetime (τ_*) as a function of mass.

6.2.6 Star Formation Rate

We adopt an empirical fit to the star formation rate per comoving volume as a function of redshift, z [236],

$$\dot{\rho}_*(z) = 0.015 \frac{(1+z)^{2.7}}{1 + [(1+z)/2.9]^{5.6}} M_\odot \text{yr}^{-1} \text{Mpc}^{-3}, \quad (6.4)$$

and truncate the extrapolation to early times at the expected formation time of the first stars [3]. We extrapolate the cosmic star formation history to the future or equivalently negative redshifts $-1 \leq z < 0$ (see, e.g. Ref. [237]) and find that the comoving star formation rate drops to less than 10^{-5} of the current rate at 56 Gyr into the future. We cut off the star formation at roughly the ratio between the current reservoir mass of cold gas in galaxies [225] and the current star formation rate per comoving volume. The resulting star formation rate as a function of time and redshift is shown in Figure 10.

6.2.7 Probability of Life on a Habitable Planet

The probability for the existence of life around a star of a particular mass m can be expressed in terms of the product between the probability that there is an Earth-mass planet in the star's habitable zone (HZ) and the probability that life emerges on such a planet: $P(\text{life}|m) = P(\text{HZ}|m)P(\text{life}|\text{HZ})$. The first factor, $P(\text{HZ}|m)$, is commonly labeled η_{Earth} in the exo-planet literature [238].

Data from the NASA Kepler mission implies η_{Earth} values in the range of $6.4^{+3.4}_{-1.1}\%$ for stars of approximately a solar mass [239–241] and $24^{+18}_{-8}\%$ for lower mass M-dwarf stars [242]. The result for solar mass stars is less robust due to lack of identified Earth-like planets at high stellar masses. Owing to the large measurement uncertainties, we assume a constant

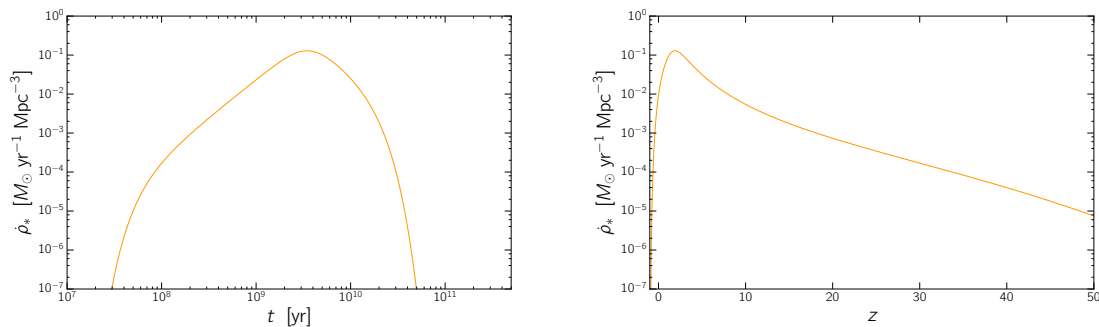


Figure 10. Star formation rate, $\dot{\rho}_*$, as a function of the cosmic time t (left panel) and redshift z (right panel), based on an extrapolation of a fitting function to existing data [236].

η_{Earth} within the range of stellar masses under consideration. The specific constant value of η_{Earth} drops out of the calculation due to the normalization factor N .

There is scope for considerable refinement in the choice of the second factor $p(\text{life}|\text{HZ})$. One could suppose that the probability of life evolving on a planet increases with the amount of time that the planet exists, or that increasing the surface area of the planet should increase the likelihood of life beginning. However, given our ignorance we will set this probability factor to a constant, an assumption which can be improved upon by statistical data from future searches for biosignatures in the molecular composition of the atmospheres of habitable planets [243–246]. In our simplified treatment, this constant value has no effect on $dP(t)/dt$ since its contribution is also cancelled by the normalization factor N .

6.3 Results

The top and bottom panels in Figure 11 show the probability per log time interval $t dP(t)/dt = dP/d\ln t$ and the cumulative probability $P(< t) = \int_0^t [dP(t')/dt'] dt'$ based on equation (6.1), for different choices of the low mass cutoff in the distribution of host stars for life-hosting planets (equally spaced in $\ln m$). The upper stellar mass cutoff has a negligible influence on $dP/d\ln t$, due to the short lifetime and low abundance of massive stars. In general, $dP/d\ln t$ cuts off roughly at the lifetime of the longest lived stars in each case, as indicated by the upper axis labels. For the full range of hydrogen-burning stars, $dP(t)/d\ln t$ peaks around the lifetime of the lowest mass stars $t \sim 10^{13}$ yr with a probability value that is a thousand times larger than for the Sun, implying that life around low mass stars in the distant future is much more likely than terrestrial life around the Sun today.

6.4 Section Summary and Implications

Figure 11 implies that the probability for life per logarithm interval of cosmic time, $dP(t)/d\ln t$, has a broad distribution in $\ln t$ and is peaked in the future, as long as life is likely around low-mass stars. High mass stars are shorter lived and less abundant and hence make a relatively small contribution to the probability distribution.

Future searches for molecular biosignatures (such as O_2 combined with CH_4) in the atmospheres of planets around low mass stars [243–245] could inform us whether life will exist at late cosmic times [247]. If we insist that life near the Sun is typical and not premature, i.e. require that the peak in $dP(t)/d\ln t$ would coincide with the lifetime of Sun-like stars at the present time, then we must conclude that the physical environments of low-mass stars

are hazardous to life (see e.g. Ref. [248]). This could result, for example, from the enhanced UV emission and flaring activity of young low-mass stars, which is capable of stripping rocky planets of their atmospheres [249].

Values of the cosmological constant below the observed one should not affect the probability distribution, as they would introduce only mild changes to the star formation history due to the modified formation history of galaxies [166, 167]. However, much larger values of the cosmological constant would suppress galaxy formation and reduce the total number of stars per comoving volume [10], hence limiting the overall likelihood for life altogether [34].

Our results provide a new perspective on the so-called “coincidence problem”, *why do we observe $\Omega_m \sim \Omega_\Lambda$?* [250] The answer comes naturally if we consider the history of Sun-like star formation, as the number of habitable planets peaks around present time for $m \sim 1M_\odot$. We note that for the majority of stars, this coincidence will not exist as $dP(t)/dt$ peaks in the future where $\Omega_m \ll \Omega_\Lambda$. The question is then, why do we find ourselves orbiting a star like the Sun now rather than a lower mass star in the future?

We derived our numerical results based on a conservative set of assumptions and guided by the latest empirical data for the various components of equation (6.1). However, the emergence of life may be sensitive to additional factors that were not included in our formulation, such as the existence of a moon to stabilize the climate on an Earth-like planet [251], the existence of asteroid belts [252], the orbital structure of the host planetary system (e.g. the existence of nearby giant planets or orbital eccentricity), the effects of a binary star companion [253], the location of the planetary system within the host galaxy [254], and the detailed properties of the host galaxy (e.g. galaxy type [234] or metallicity [106]), including the environmental effects of quasars, γ -ray bursts [255] or the hot gas in clusters of galaxies. These additional factors are highly uncertain and complicated to model and were ignored for simplicity in our analysis.

The probability distribution $dP(t)/d \ln t$ is of particular importance for studies attempting to gauge the level of fine-tuning required for the cosmological or fundamental physics parameters that would allow life to emerge in our Universe.

Acknowledgments

I thank my collaborators on the work described in this chapter, namely Rafael Batista, Shmuel Bialy, Natalie Mashian, David Sloan and Amiel Sternberg.

References

- [1] J. F. Kasting, D. P. Whitmire and R. T. Reynolds, *Habitable Zones around Main Sequence Stars*, *Icarus* **101** (Jan., 1993) 108–128.
- [2] J. Kasting, *How to Find a Habitable Planet*. Princeton University Press, 2010.
- [3] A. Loeb, *The habitable epoch of the early Universe*, *International Journal of Astrobiology* **13** (Sept., 2014) 337–339, [1312.0613].
- [4] E. L. Schaller and M. E. Brown, *Volatile Loss and Retention on Kuiper Belt Objects*, *The Astrophysical Journal Letters* **659** (Apr., 2007) L61–L64.
- [5] A. Loeb and S. R. Furlanetto, *The First Galaxies in the Universe*. 2013.
- [6] A. Fialkov, R. Barkana, D. Tseliakhovich and C. M. Hirata, *Impact of the relative motion between the dark matter and baryons on the first stars: semi-analytical modelling*, *Monthly Notices of the Royal Astronomical Society* **424** (Aug., 2012) 1335–1345, [1110.2111].

- [7] S. Naoz, S. Noter and R. Barkana, *The first stars in the Universe*, *Monthly Notices of the Royal Astronomical Society* **373** (Nov., 2006) L98–L102, [[astro-ph/0604050](#)].
- [8] N. Mashian and A. Loeb, *CEMP stars: possible hosts to carbon planets in the early universe*, *Monthly Notices of the Royal Astronomical Society* (May, 2016) , [[1603.06943](#)].
- [9] S. Bialy, A. Sternberg and A. Loeb, *Water Formation During the Epoch of First Metal Enrichment*, *The Astrophysical Journal Letters* **804** (May, 2015) L29, [[1503.03475](#)].
- [10] A. Loeb, *An observational test for the anthropic origin of the cosmological constant*, *Journal of Cosmology and Astroparticle Physics* **5** (May, 2006) 009, [[astro-ph/0604242](#)].
- [11] A. Loeb, R. Batista and D. Sloan, *The Relative Likelihood of Life as a Function of Cosmic Time*, *Journal of Cosmology and Astroparticle Physics* (2016) TBD, [[1606.08448](#)].
- [12] D. J. Fixsen, *The Temperature of the Cosmic Microwave Background*, *The Astrophysical Journal* **707** (Dec., 2009) 916–920, [[0911.1955](#)].
- [13] W. W. Ober, M. F. El Eid and K. J. Fricke, *Evolution of Massive Pregalactic Stars - Part Two - Nucleosynthesis in Pair Creation Supernovae and Pregalactic Enrichment*, *Astronomy and Astrophysics* **119** (Mar., 1983) 61.
- [14] A. Heger and S. E. Woosley, *The Nucleosynthetic Signature of Population III*, *The Astrophysical Journal* **567** (Mar., 2002) 532–543, [[astro-ph/0107037](#)].
- [15] V. Bromm and R. B. Larson, *The First Stars*, *Annual Reviews of Astronomy and Astrophysics* **42** (Sept., 2004) 79–118, [[astro-ph/0311019](#)].
- [16] M. F. El Eid, K. J. Fricke and W. W. Ober, *Evolution of massive pregalactic stars. I - Hydrogen and helium burning. II - Nucleosynthesis in pair creation supernovae and pregalactic enrichment*, *Astronomy and Astrophysics* **119** (Mar., 1983) 54–68.
- [17] V. Bromm, R. P. Kudritzki and A. Loeb, *Generic Spectrum and Ionization Efficiency of a Heavy Initial Mass Function for the First Stars*, *The Astrophysical Journal* **552** (May, 2001) 464–472, [[astro-ph/0007248](#)].
- [18] Planck Collaboration, P. A. R. Ade, N. Aghanim, M. Arnaud, M. Ashdown, J. Aumont et al., *Planck 2015 results. XIII. Cosmological parameters*, *ArXiv e-prints* (Feb., 2015) , [[1502.01589](#)].
- [19] L. Anderson, É. Aubourg, S. Bailey and e. a. Beutler, F., *The clustering of galaxies in the SDSS-III Baryon Oscillation Spectroscopic Survey: baryon acoustic oscillations in the Data Releases 10 and 11 Galaxy samples*, *Monthly Notices of the Royal Astronomical Society* **441** (June, 2014) 24–62, [[1312.4877](#)].
- [20] S. Shandera, A. Mantz, D. Rapetti and S. W. Allen, *X-ray cluster constraints on non-Gaussianity*, *Journal of Cosmology and Astroparticle Physics* **8** (Aug., 2013) 004, [[1304.1216](#)].
- [21] J. R. Pritchard and A. Loeb, *21 cm cosmology in the 21st century*, *Reports on Progress in Physics* **75** (Aug., 2012) 086901, [[1109.6012](#)].
- [22] Z. Haiman, A. A. Thoul and A. Loeb, *Cosmological Formation of Low-Mass Objects*, *The Astrophysical Journal* **464** (June, 1996) 523, [[astro-ph/9507111](#)].
- [23] M. Tegmark, J. Silk, M. J. Rees, A. Blanchard, T. Abel and F. Palla, *How Small Were the First Cosmological Objects?*, *The Astrophysical Journal* **474** (Jan., 1997) 1, [[astro-ph/9603007](#)].
- [24] C. M. Hirata and N. Padmanabhan, *Cosmological production of H₂ before the formation of the first galaxies*, *Monthly Notices of the Royal Astronomical Society* **372** (Nov., 2006) 1175–1186, [[astro-ph/0606437](#)].

- [25] D. Tseliakhovich, R. Barkana and C. M. Hirata, *Suppression and spatial variation of early galaxies and minihaloes*, *Monthly Notices of the Royal Astronomical Society* **418** (Dec., 2011) 906–915, [[1012.2574](#)].
- [26] R. K. Sheth and G. Tormen, *Large-scale bias and the peak background split*, *Monthly Notices of the Royal Astronomical Society* **308** (Sept., 1999) 119–126, [[astro-ph/9901122](#)].
- [27] M. LoVerde and K. M. Smith, *The non-Gaussian halo mass function with f_{NL} , g_{NL} and τ_{NL}* , *Journal of Cosmology and Astroparticle Physics* **8** (Aug., 2011) 003, [[1102.1439](#)].
- [28] U. Maio, R. Salvaterra, L. Moscardini and B. Ciardi, *Counts of high-redshift GRBs as probes of primordial non-Gaussianities*, *Monthly Notices of the Royal Astronomical Society* **426** (Nov., 2012) 2078–2088, [[1209.2250](#)].
- [29] M. Musso and R. K. Sheth, *The excursion set approach in non-Gaussian random fields*, *Monthly Notices of the Royal Astronomical Society* **439** (Apr., 2014) 3051–3063, [[1305.0724](#)].
- [30] Planck Collaboration, P. A. R. Ade, N. Aghanim, M. Arnaud, F. Arroja, M. Ashdown et al., *Planck 2015 results. XVII. Constraints on primordial non-Gaussianity*, *ArXiv e-prints* (Feb., 2015) , [[1502.01592](#)].
- [31] J. Maldacena, *Non-gaussian features of primordial fluctuations in single field inflationary models*, *Journal of High Energy Physics* **5** (May, 2003) 013, [[astro-ph/0210603](#)].
- [32] D. J. Stevenson, *Life-sustaining planets in interstellar space?*, *Nature* **400** (July, 1999) 32.
- [33] R. Pierrehumbert and E. Gaidos, *Hydrogen Greenhouse Planets Beyond the Habitable Zone*, *The Astrophysical Journal Letters* **734** (June, 2011) L13, [[1105.0021](#)].
- [34] S. Weinberg, *Anthropic bound on the cosmological constant*, *Physical Review Letters* **59** (Nov., 1987) 2607–2610.
- [35] J. Garriga and A. Vilenkin, *Anthropic Prediction for Λ and the Q Catastrophe*, *Progress of Theoretical Physics Supplement* **163** (2006) 245–257, [[hep-th/0508005](#)].
- [36] M. Tegmark, A. Aguirre, M. J. Rees and F. Wilczek, *Dimensionless constants, cosmology, and other dark matters*, *Physical Review D* **73** (Jan., 2006) 023505, [[astro-ph/0511774](#)].
- [37] R. Barkana and A. Loeb, *In the beginning: the first sources of light and the reionization of the universe*, *Physics Reports* **349** (July, 2001) 125–238, [[astro-ph/0010468](#)].
- [38] N. Yoshida, T. Abel, L. Hernquist and N. Sugiyama, *Simulations of Early Structure Formation: Primordial Gas Clouds*, *The Astrophysical Journal* **592** (Aug., 2003) 645–663, [[astro-ph/0301645](#)].
- [39] V. Bromm and A. Loeb, *The formation of the first low-mass stars from gas with low carbon and oxygen abundances*, *Nature* **425** (Oct., 2003) 812–814, [[astro-ph/0310622](#)].
- [40] A. Frebel, J. L. Johnson and V. Bromm, *Probing the formation of the first low-mass stars with stellar archaeology*, *Monthly Notices of the Royal Astronomical Society* **380** (Sept., 2007) L40–L44, [[astro-ph/0701395](#)].
- [41] P. C. Clark, S. C. O. Glover and R. S. Klessen, *The First Stellar Cluster*, *The Astrophysical Journal* **672** (Jan., 2008) 757–764.
- [42] J. C. B. Papaloizou and C. Terquem, *Planet formation and migration*, *Reports on Progress in Physics* **69** (Jan., 2006) 119–180, [[astro-ph/0510487](#)].
- [43] M. Janson, M. Bonavita, H. Klahr, D. Lafrenière, R. Jayawardhana and H. Zinnecker, *High-contrast Imaging Search for Planets and Brown Dwarfs around the Most Massive Stars in the Solar Neighborhood*, *The Astrophysical Journal* **736** (Aug., 2011) 89, [[1105.2577](#)].
- [44] K. Kornet, P. Bodenheimer, M. Różyczka and T. F. Stepinski, *Formation of giant planets in disks with different metallicities*, *Astronomy and Astrophysics* **430** (Feb., 2005) 1133–1138, [[astro-ph/0410112](#)].

- [45] A. Johansen, A. Youdin and M.-M. Mac Low, *Particle Clumping and Planetesimal Formation Depend Strongly on Metallicity*, *The Astrophysical Journal* **704** (Oct., 2009) L75–L79, [[0909.0259](#)].
- [46] C. Yasui, N. Kobayashi, A. T. Tokunaga, M. Saito and C. Tokoku, *The Lifetime of Protoplanetary Disks in a Low-metallicity Environment*, *The Astrophysical Journal* **705** (Nov., 2009) 54–63, [[0908.4026](#)].
- [47] B. Ercolano and C. J. Clarke, *Metallicity, planet formation and disc lifetimes*, *Monthly Notices of the Royal Astronomical Society* **402** (Mar., 2010) 2735–2743, [[0910.5110](#)].
- [48] T. C. Beers, G. W. Preston and S. A. Shectman, *A search for stars of very low metal abundance. I*, *The Astronomical Journal* **90** (Oct., 1985) 2089–2102.
- [49] L. Wisotzki, T. Koehler, D. Groote and D. Reimers, *The Hamburg/ESO survey for bright QSOs. I. Survey design and candidate selection procedure.*, *Astronomy and Astrophysics Supp.* **115** (Feb., 1996) 227.
- [50] N. Christlieb, T. Schörck, A. Frebel, T. C. Beers, L. Wisotzki and D. Reimers, *The stellar content of the Hamburg/ESO survey. IV. Selection of candidate metal-poor stars*, *Astronomy and Astrophysics* **484** (June, 2008) 721–732, [[0804.1520](#)].
- [51] D. G. York, J. Adelman and e. a. Anderson, J. E., *The Sloan Digital Sky Survey: Technical Summary*, *The Astronomical Journal* **120** (Sept., 2000) 1579–1587, [[astro-ph/0006396](#)].
- [52] B. Yanny, C. Rockosi, H. J. Newberg and e. a. Knapp, G. R., *SEGUE: A Spectroscopic Survey of 240,000 Stars with $g = 14$ –20*, *The Astronomical Journal* **137** (May, 2009) 4377–4399, [[0902.1781](#)].
- [53] W. Aoki, T. C. Beers, N. Christlieb, J. E. Norris, S. G. Ryan and S. Tsangarides, *Carbon-enhanced Metal-poor Stars. I. Chemical Compositions of 26 Stars*, *The Astrophysical Journal* **655** (Jan., 2007) 492–521, [[astro-ph/0609702](#)].
- [54] D. Carollo, T. C. Beers, J. Bovy, T. Sivarani, J. E. Norris, K. C. Freeman et al., *Carbon-enhanced Metal-poor Stars in the Inner and Outer Halo Components of the Milky Way*, *The Astrophysical Journal* **744** (Jan., 2012) 195, [[1103.3067](#)].
- [55] J. E. Norris, D. Yong, M. S. Bessell, N. Christlieb, M. Asplund, G. Gilmore et al., *The Most Metal-poor Stars. IV. The Two Populations with $[Fe/H] < \sim -3.0$* , *The Astrophysical Journal* **762** (Jan., 2013) 28, [[1211.3157](#)].
- [56] T. C. Beers and N. Christlieb, *The Discovery and Analysis of Very Metal-Poor Stars in the Galaxy*, *Annual Reviews of Astronomy and Astrophysics* **43** (Sept., 2005) 531–580.
- [57] A. Frebel and J. E. Norris, *Near-Field Cosmology with Extremely Metal-Poor Stars*, *Annual Reviews of Astronomy and Astrophysics* **53** (Aug., 2015) 631–688, [[1501.06921](#)].
- [58] M. J. Kuchner and S. Seager, *Extrasolar Carbon Planets*, *ArXiv Astrophysics e-prints* (Apr., 2005) , [[astro-ph/0504214](#)].
- [59] J. C. Bond, D. P. O’Brien and D. S. Lauretta, *The Compositional Diversity of Extrasolar Terrestrial Planets. I. In Situ Simulations*, *The Astrophysical Journal* **715** (June, 2010) 1050–1070, [[1004.0971](#)].
- [60] J. C. Carter-Bond, D. P. O’Brien, E. Delgado Mena, G. Israelian, N. C. Santos and J. I. González Hernández, *Low Mg/Si Planetary Host Stars and Their Mg-depleted Terrestrial Planets*, *The Astrophysical Journal* **747** (Mar., 2012) L2, [[1201.1939](#)].
- [61] J. C. Carter-Bond, D. P. O’Brien and S. N. Raymond, *The Compositional Diversity of Extrasolar Terrestrial Planets. II. Migration Simulations*, *The Astrophysical Journal* **760** (Nov., 2012) 44, [[1209.5125](#)].

- [62] J. W. Larimer, *The effect of C/O ratio on the condensation of planetary material*, *Ge. Co. A.* **39** (Mar., 1975) 389–392.
- [63] N. Madhusudhan, J. Harrington and e. a. Stevenson, K. B., *A high C/O ratio and weak thermal inversion in the atmosphere of exoplanet WASP-12b*, *Nature* **469** (Jan., 2011) 64–67, [[1012.1603](#)].
- [64] N. Madhusudhan, K. K. M. Lee and O. Mousis, *A Possible Carbon-rich Interior in Super-Earth 55 Cancri e*, *The Astrophysical Journal* **759** (Nov., 2012) L40, [[1210.2720](#)].
- [65] M. Asplund, N. Grevesse, A. J. Sauval and P. Scott, *The Chemical Composition of the Sun*, *Annual Reviews of Astronomy and Astrophysics* **47** (Sept., 2009) 481–522, [[0909.0948](#)].
- [66] W. Aoki, *Carbon-Enhanced Metal-Poor (CEMP) stars*, in *Chemical Abundances in the Universe: Connecting First Stars to Planets* (K. Cunha, M. Spite and B. Barbuy, eds.), vol. 265 of *IAU Symposium*, pp. 111–116, Mar., 2010. DOI.
- [67] H. Umeda and K. Nomoto, *First-generation black-hole-forming supernovae and the metal abundance pattern of a very iron-poor star*, *Nature* **422** (Apr., 2003) 871–873, [[astro-ph/0301315](#)].
- [68] H. Umeda and K. Nomoto, *Variations in the Abundance Pattern of Extremely Metal-Poor Stars and Nucleosynthesis in Population III Supernovae*, *The Astrophysical Journal* **619** (Jan., 2005) 427–445, [[astro-ph/0308029](#)].
- [69] M. de Bannassuti, R. Schneider, R. Valiante and S. Salvadori, *Decoding the stellar fossils of the dusty Milky Way progenitors*, *Monthly Notices of the Royal Astronomical Society* **445** (Dec., 2014) 3039–3054, [[1409.5798](#)].
- [70] R. J. Cooke and P. Madau, *Carbon-enhanced Metal-poor Stars: Relics from the Dark Ages*, *The Astrophysical Journal* **791** (Aug., 2014) 116, [[1405.7369](#)].
- [71] N. Iwamoto, H. Umeda, N. Tominaga, K. Nomoto and K. Maeda, *The First Chemical Enrichment in the Universe and the Formation of Hyper Metal-Poor Stars*, *Science* **309** (July, 2005) 451–453, [[astro-ph/0505524](#)].
- [72] C. C. Joggerst, S. E. Woosley and A. Heger, *Mixing in Zero- and Solar-Metallicity Supernovae*, *The Astrophysical Journal* **693** (Mar., 2009) 1780–1802, [[0810.5142](#)].
- [73] D. Yong, J. E. Norris, M. S. Bessell, N. Christlieb, M. Asplund, T. C. Beers et al., *The Most Metal-poor Stars. III. The Metallicity Distribution Function and Carbon-enhanced Metal-poor Fraction*, *The Astrophysical Journal* **762** (Jan., 2013) 27, [[1208.3016](#)].
- [74] S. C. Keller, M. S. Bessell, A. Frebel and e. a. Casey, A. R., *A single low-energy, iron-poor supernova as the source of metals in the star SMSS J031300.36-670839.3*, *Nature* **506** (Feb., 2014) 463–466, [[1402.1517](#)].
- [75] M. N. Ishigaki, N. Tominaga, C. Kobayashi and K. Nomoto, *Faint Population III Supernovae as the Origin of the Most Iron-poor Stars*, *The Astrophysical Journal* **792** (Sept., 2014) L32, [[1404.4817](#)].
- [76] S. Marassi, G. Chiaki, R. Schneider, M. Limongi, K. Omukai, T. Nozawa et al., *The Origin of the Most Iron-poor Star*, *The Astrophysical Journal* **794** (Oct., 2014) 100, [[1409.4424](#)].
- [77] S. Marassi, R. Schneider, M. Limongi, A. Chieffi, M. Bocchio and S. Bianchi, *The metal and dust yields of the first massive stars*, *Monthly Notices of the Royal Astronomical Society* **454** (Dec., 2015) 4250–4266, [[1509.08923](#)].
- [78] N. Tominaga, N. Iwamoto and K. Nomoto, *Abundance Profiling of Extremely Metal-poor Stars and Supernova Properties in the Early Universe*, *The Astrophysical Journal* **785** (Apr., 2014) 98, [[1309.6734](#)].

- [79] P. Bonifacio, E. Caffau, M. Spite and e. a. Limongi, M., *TOPoS . II. On the bimodality of carbon abundance in CEMP stars Implications on the early chemical evolution of galaxies*, *Astronomy and Astrophysics* **579** (July, 2015) A28, [[1504.05963](#)].
- [80] E. Zinner, *Leonard Award Address—Trends in the study of presolar dust grains from primitive meteorites*, *Meteoritics and Planetary Science* **33** (July, 1998) 549–564.
- [81] L. B. Lucy, I. J. Danziger, C. Gouffes and P. Bouchet, *Dust Condensation in the Ejecta of SN 1987 A*, in *IAU Colloq. 120: Structure and Dynamics of the Interstellar Medium* (G. Tenorio-Tagle, M. Moles and J. Melnick, eds.), vol. 350 of *Lecture Notes in Physics*, Berlin Springer Verlag, p. 164, 1989. DOI.
- [82] R. Indebetouw, M. Matsuura, E. Dwek and e. a. Zanardo, G., *Dust Production and Particle Acceleration in Supernova 1987A Revealed with ALMA*, *The Astrophysical Journal* **782** (Feb., 2014) L2, [[1312.4086](#)].
- [83] A. Elmhamdi, I. J. Danziger, N. Chugai, A. Pastorello, M. Turatto, E. Cappellaro et al., *Photometry and spectroscopy of the Type IIP SN 1999em from outburst to dust formation*, *Monthly Notices of the Royal Astronomical Society* **338** (Feb., 2003) 939–956, [[astro-ph/0209623](#)].
- [84] L. Dunne, S. Eales, R. Ivison, H. Morgan and M. Edmunds, *Type II supernovae as a significant source of interstellar dust*, *Nature* **424** (July, 2003) 285–287, [[astro-ph/0307320](#)].
- [85] T. Kozasa, H. Hasegawa and K. Nomoto, *Formation of dust grains in the ejecta of SN 1987A*, *The Astrophysical Journal* **344** (Sept., 1989) 325–331.
- [86] P. Todini and A. Ferrara, *Dust formation in primordial Type II supernovae*, *Monthly Notices of the Royal Astronomical Society* **325** (Aug., 2001) 726–736, [[astro-ph/0009176](#)].
- [87] T. Nozawa, T. Kozasa, H. Umeda, K. Maeda and K. Nomoto, *Dust in the Early Universe: Dust Formation in the Ejecta of Population III Supernovae*, *The Astrophysical Journal* **598** (Dec., 2003) 785–803, [[astro-ph/0307108](#)].
- [88] M. E. Kress and A. G. G. M. Tielens, *The role of Fischer-Tropsch catalysis in solar nebula chemistry*, *Meteoritics and Planetary Science* **36** (Jan., 2001) 75–92.
- [89] J. J. Lissauer, *Planet formation*, *Annual Reviews of Astronomy and Astrophysics* **31** (1993) 129–174.
- [90] S. V. W. Beckwith, T. Henning and Y. Nakagawa, *Dust Properties and Assembly of Large Particles in Protoplanetary Disks*, *Protostars and Planets IV* (May, 2000) 533, [[astro-ph/9902241](#)].
- [91] M. Nagasawa, E. W. Thommes, S. J. Kenyon, B. C. Bromley and D. N. C. Lin, *The Diverse Origins of Terrestrial-Planet Systems*, *Protostars and Planets V* (2007) 639–654.
- [92] P. J. Armitage, *Astrophysics of Planet Formation*. 2010.
- [93] U. Gorti and D. Hollenbach, *Photoevaporation of Circumstellar Disks By Far-Ultraviolet, Extreme-Ultraviolet and X-Ray Radiation from the Central Star*, *The Astrophysical Journal* **690** (Jan., 2009) 1539–1552, [[0809.1494](#)].
- [94] B. Ercolano, C. J. Clarke and J. J. Drake, *X-Ray Irradiated Protoplanetary Disk Atmospheres. II. Predictions from Models in Hydrostatic Equilibrium*, *The Astrophysical Journal* **699** (July, 2009) 1639–1649, [[0905.1001](#)].
- [95] S. M. Andrews, D. J. Wilner, A. M. Hughes, C. Qi and C. P. Dullemond, *Protoplanetary Disk Structures in Ophiuchus*, *The Astrophysical Journal* **700** (Aug., 2009) 1502–1523, [[0906.0730](#)].
- [96] S. M. Andrews, D. J. Wilner, A. M. Hughes, C. Qi and C. P. Dullemond, *Protoplanetary Disk Structures in Ophiuchus. II. Extension to Fainter Sources*, *The Astrophysical Journal* **723** (Nov., 2010) 1241–1254, [[1007.5070](#)].

- [97] C. P. Dullemond and C. Dominik, *Dust coagulation in protoplanetary disks: A rapid depletion of small grains*, *Astronomy and Astrophysics* **434** (May, 2005) 971–986, [[astro-ph/0412117](#)].
- [98] N. Christlieb, M. S. Bessell, T. C. Beers, B. Gustafsson, A. Korn, P. S. Barklem et al., *A stellar relic from the early Milky Way*, *Nature* **419** (Oct., 2002) 904–906, [[astro-ph/0211274](#)].
- [99] S. M. Andrews and J. P. Williams, *Circumstellar Dust Disks in Taurus-Auriga: The Submillimeter Perspective*, *The Astrophysical Journal* **631** (Oct., 2005) 1134–1160, [[astro-ph/0506187](#)].
- [100] A. P. Ji, A. Frebel and V. Bromm, *The Chemical Imprint of Silicate Dust on the Most Metal-poor Stars*, *The Astrophysical Journal* **782** (Feb., 2014) 95, [[1307.2239](#)].
- [101] N. Christlieb, B. Gustafsson, A. J. Korn, P. S. Barklem, T. C. Beers, M. S. Bessell et al., *HE 0107-5240, a Chemically Ancient Star. I. A Detailed Abundance Analysis*, *The Astrophysical Journal* **603** (Mar., 2004) 708–728, [[astro-ph/0311173](#)].
- [102] R. Collet, M. Asplund and R. Trampedach, *The Chemical Compositions of the Extreme Halo Stars HE 0107-5240 and HE 1327-2326 Inferred from Three-dimensional Hydrodynamical Model Atmospheres*, *The Astrophysical Journal* **644** (June, 2006) L121–L124, [[astro-ph/0605219](#)].
- [103] B. Plez and J. G. Cohen, *Analysis of the carbon-rich very metal-poor dwarf G77-61*, *Astronomy and Astrophysics* **434** (May, 2005) 1117–1124, [[astro-ph/0501535](#)].
- [104] T. C. Beers, T. Sivarani, B. Marsteller, Y. Lee, S. Rossi and B. Plez, *Near-Infrared Spectroscopy of Carbon-Enhanced Metal-Poor Stars. I. A SOAR/OSIRIS Pilot Study*, *The Astronomical Journal* **133** (Mar., 2007) 1193–1203, [[astro-ph/0611827](#)].
- [105] I. U. Roederer, G. W. Preston, I. B. Thompson, S. A. Shectman, C. Sneden, G. S. Burley et al., *A Search for Stars of Very Low Metal Abundance. VI. Detailed Abundances of 313 Metal-poor Stars*, *The Astronomical Journal* **147** (June, 2014) 136, [[1403.6853](#)].
- [106] J. L. Johnson and H. Li, *The First Planets: The Critical Metallicity for Planet Formation*, *The Astrophysical Journal* **751** (June, 2012) 81, [[1203.4817](#)].
- [107] H. Kobayashi, H. Kimura, S.-i. Watanabe, T. Yamamoto and S. Müller, *Sublimation temperature of circumstellar dust particles and its importance for dust ring formation*, *Earth, Planets, and Space* **63** (Oct., 2011) 1067–1075, [[1104.5627](#)].
- [108] C. C. Dahn, J. Liebert, R. G. Kron, H. Spinrad and P. M. Hintzen, *G77-61 - A dwarf carbon star*, *The Astrophysical Journal* **216** (Sept., 1977) 757–766.
- [109] J. E. Norris, S. G. Ryan and T. C. Beers, *Extremely Metal-poor Stars. The Carbon-rich, Neutron Capture Element-poor Object CS 22957-027*, *The Astrophysical Journal* **489** (Nov., 1997) L169.
- [110] H. S. Zepolsky and E. E. Salpeter, *The Mass-Radius Relation for Cold Spheres of Low Mass*, *The Astrophysical Journal* **158** (Nov., 1969) 809.
- [111] A. Léger, F. Selsis, C. Sotin, T. Guillot, D. Despois, D. Mawet et al., *A new family of planets? “Ocean-Planets”*, *Icarus* **169** (June, 2004) 499–504, [[astro-ph/0308324](#)].
- [112] D. Valencia, R. J. O’Connell and D. Sasselo, *Internal structure of massive terrestrial planets*, *Icarus* **181** (Apr., 2006) 545–554, [[astro-ph/0511150](#)].
- [113] J. J. Fortney, M. S. Marley and J. W. Barnes, *Planetary Radii across Five Orders of Magnitude in Mass and Stellar Insolation: Application to Transits*, *The Astrophysical Journal* **659** (Apr., 2007) 1661–1672, [[astro-ph/0612671](#)].
- [114] S. Seager, M. Kuchner, C. A. Hier-Majumder and B. Militzer, *Mass-Radius Relationships for Solid Exoplanets*, *The Astrophysical Journal* **669** (Nov., 2007) 1279–1297, [[0707.2895](#)].

- [115] A. G. G. M. Tielens, C. G. Seab, D. J. Hollenbach and C. F. McKee, *Shock processing of interstellar dust - Diamonds in the sky*, *The Astrophysical Journal* **319** (Aug., 1987) L109–L113.
- [116] R. Papoular, J. Conard, O. Guillois, I. Nenner, C. Reynaud and J.-N. Rouzaud, *A comparison of solid-state carbonaceous models of cosmic dust.*, *Astronomy and Astrophysics* **315** (Nov., 1996) 222–236.
- [117] K. Takai, M. Oga, H. Sato, T. Enoki, Y. Ohki, A. Taomoto et al., *Structure and electronic properties of a nongraphitic disordered carbon system and its heat-treatment effects*, *Physical Review B* **67** (June, 2003) 214202.
- [118] F. Birch, *Finite Elastic Strain of Cubic Crystals*, *Physical Review* **71** (June, 1947) 809–824.
- [119] M. Hanfland, H. Beister and K. Syassen, *Graphite under pressure: Equation of state and first-order Raman modes*, *Physical Review B* **39** (June, 1989) 12598–12603.
- [120] S. Naka, K. Horii, Y. Takeda and T. Hanawa, *Direct conversion of graphite to diamond under static pressure*, *Nature* **259** (Jan., 1976) 38–39.
- [121] P. Vinet, J. Ferrante, J. H. Rose and J. R. Smith, *Compressibility of solids*, *J. G. R.* **92** (Aug., 1987) 9319–9325.
- [122] P. Vinet, J. H. Rose, J. Ferrante and J. R. Smith, *Universal features of the equation of state of solids*, *Journal of Physics Condensed Matter* **1** (Mar., 1989) 1941–1963.
- [123] A. Dewaele, F. Datchi, P. Loubeyre and M. Mezouar, *High pressure-high temperature equations of state of neon and diamond*, *Physical Review B* **77** (Mar., 2008) 094106.
- [124] E. E. Salpeter and H. S. Zapolsky, *Theoretical High-Pressure Equations of State including Correlation Energy*, *Physical Review* **158** (June, 1967) 876–886.
- [125] W. B. Hubbard, *Planetary interiors*. 1984.
- [126] W. J. Borucki, E. W. Dunham, D. G. Koch, W. D. Cochran, J. D. Rose, D. K. Cullers et al., *FRESIP: A Mission to Determine the Character and Frequency of Extra-Solar Planets Around Solar-Like Stars*, *Astrophysics and Space Science* **241** (Mar., 1996) 111–134.
- [127] S. Seager and G. Mallén-Ornelas, *A Unique Solution of Planet and Star Parameters from an Extrasolar Planet Transit Light Curve*, *The Astrophysical Journal* **585** (Mar., 2003) 1038–1055, [[astro-ph/0206228](#)].
- [128] C. A. Beichman, T. Greene and J. Krist, *Future Observations of Transits and Light Curves from Space*, in *Transiting Planets* (F. Pont, D. Sasselov and M. J. Holman, eds.), vol. 253 of *IAU Symposium*, pp. 319–328, Feb., 2009. DOI.
- [129] J. N. Winn and D. C. Fabrycky, *The Occurrence and Architecture of Exoplanetary Systems*, *Annual Reviews of Astronomy and Astrophysics* **53** (Aug., 2015) 409–447, [[1410.4199](#)].
- [130] S. R. Kane, *Detectability of exoplanetary transits from radial velocity surveys*, *Monthly Notices of the Royal Astronomical Society* **380** (Oct., 2007) 1488–1496, [[0706.3704](#)].
- [131] J. M. Hahn and R. Malhotra, *Orbital Evolution of Planets Embedded in a Planetesimal Disk*, *The Astronomical Journal* **117** (June, 1999) 3041–3053, [[astro-ph/9902370](#)].
- [132] D. Veras, J. R. Crepp and E. B. Ford, *Formation, Survival, and Detectability of Planets Beyond 100 AU*, *The Astrophysical Journal* **696** (May, 2009) 1600–1611, [[0902.2779](#)].
- [133] A. Niedzielski, G. Nowak, M. Adamów and A. Wolszczan, *Substellar-mass Companions to the K-dwarf BD+14 4559 and the K-giants HD 240210 and BD+20 2457*, *The Astrophysical Journal* **707** (Dec., 2009) 768–777, [[0906.1804](#)].
- [134] G. Gonzalez, D. Brownlee and P. Ward, *The Galactic Habitable Zone: Galactic Chemical Evolution*, *Icarus* **152** (July, 2001) 185–200, [[astro-ph/0103165](#)].

- [135] R. Pinotti, L. Arany-Prado, W. Lyra and G. F. Porto de Mello, *A link between the semimajor axis of extrasolar gas giant planets and stellar metallicity*, *Monthly Notices of the Royal Astronomical Society* **364** (Nov., 2005) 29–36, [[astro-ph/0501313](#)].
- [136] E. F. van Dishoeck, E. Herbst and D. A. Neufeld, *Interstellar Water Chemistry: From Laboratory to Observations*, *Chemical Reviews* **113** (Dec., 2013) 9043–9085, [[1312.4684](#)].
- [137] E. Herbst and W. Klemperer, *The Formation and Depletion of Molecules in Dense Interstellar Clouds*, *The Astrophysical Journal* **185** (Oct., 1973) 505–534.
- [138] D. Hollenbach, M. J. Kaufman, E. A. Bergin and G. J. Melnick, *Water, O₂, and Ice in Molecular Clouds*, *The Astrophysical Journal* **690** (Jan., 2009) 1497–1521, [[0809.1642](#)].
- [139] P. Sonnentrucker, D. A. Neufeld and e. a. Phillips, T. G., *Detection of hydrogen fluoride absorption in diffuse molecular clouds with Herschel/HIFI: an ubiquitous tracer of molecular gas*, *Astronomy and Astrophysics* **521** (Oct., 2010) L12, [[1007.2148](#)].
- [140] R. R. Monje, M. Emprechtinger, T. G. Phillips, D. C. Lis, P. F. Goldsmith, E. A. Bergin et al., *Herschel/HIFI Observations of Hydrogen Fluoride Toward Sagittarius B2(M)*, *The Astrophysical Journal* **734** (June, 2011) L23, [[1108.3104](#)].
- [141] P. Sonnentrucker, D. A. Neufeld, M. Gerin, M. De Luca, N. Indriolo, D. C. Lis et al., *Herschel Observations Reveal Anomalous Molecular Abundances toward the Galactic Center*, *The Astrophysical Journal* **763** (Jan., 2013) L19.
- [142] B. T. Draine, W. G. Roberge and A. Dalgarno, *Magnetohydrodynamic shock waves in molecular clouds*, *The Astrophysical Journal* **264** (Jan., 1983) 485–507.
- [143] M. J. Kaufman and D. A. Neufeld, *Far-Infrared Water Emission from Magnetohydrodynamic Shock Waves*, *The Astrophysical Journal* **456** (Jan., 1996) 611.
- [144] K. Omukai, T. Tsuribe, R. Schneider and A. Ferrara, *Thermal and Fragmentation Properties of Star-forming Clouds in Low-Metallicity Environments*, *The Astrophysical Journal* **626** (June, 2005) 627–643, [[astro-ph/0503010](#)].
- [145] S. C. O. Glover and P. C. Clark, *Molecular cooling in the diffuse interstellar medium*, *Monthly Notices of the Royal Astronomical Society* **437** (Jan., 2014) 9–20, [[1305.7365](#)].
- [146] D. Hollenbach, M. J. Kaufman, D. Neufeld, M. Wolfire and J. R. Goicoechea, *The Chemistry of Interstellar OH⁺, H₂O⁺, and H₃O⁺: Inferring the Cosmic-Ray Ionization Rates from Observations of Molecular Ions*, *The Astrophysical Journal* **754** (Aug., 2012) 105, [[1205.6446](#)].
- [147] E. Bayet, S. Viti, D. A. Williams, J. M. C. Rawlings and T. Bell, *Molecular Tracers of Pdr-Dominated Galaxies*, *The Astrophysical Journal* **696** (May, 2009) 1466–1477, [[0903.3191](#)].
- [148] E. M. Penteado, H. M. Cuppen and H. J. Rocha-Pinto, *Modelling the chemical evolution of molecular clouds as a function of metallicity*, *Monthly Notices of the Royal Astronomical Society* **439** (Apr., 2014) 3616–3629, [[1403.0765](#)].
- [149] S. Bialy and A. Sternberg, *CO/H₂, C/CO, OH/CO, and OH/O₂ in dense interstellar gas: from high ionization to low metallicity*, *Monthly Notices of the Royal Astronomical Society* **450** (July, 2015) 4424–4445, [[1409.6724](#)].
- [150] B. T. Draine, *Physics of the Interstellar and Intergalactic Medium*. 2011.
- [151] A. Dalgarno, *Interstellar Chemistry Special Feature: The galactic cosmic ray ionization rate*, *Proceedings of the National Academy of Science* **103** (Aug., 2006) 12269–12273.
- [152] N. Indriolo and B. J. McCall, *Investigating the Cosmic-Ray Ionization Rate in the Galactic Diffuse Interstellar Medium through Observations of H⁺₃*, *The Astrophysical Journal* **745** (Jan., 2012) 91, [[1111.6936](#)].
- [153] B. T. Draine and F. Bertoldi, *Structure of Stationary Photodissociation Fronts*, *The Astrophysical Journal* **468** (Sept., 1996) 269, [[astro-ph/9603032](#)].

- [154] A. Sternberg, F. Le Petit, E. Roueff and J. Le Bourlot, *H I-to-H₂ Transitions and H I Column Densities in Galaxy Star-forming Regions*, *The Astrophysical Journal* **790** (July, 2014) 10, [[1404.5042](#)].
- [155] D. McElroy, C. Walsh, A. J. Markwick, M. A. Cordiner, K. Smith and T. J. Millar, *The UMIST database for astrochemistry 2012*, *Astronomy and Astrophysics* **550** (Feb., 2013) A36, [[1212.6362](#)].
- [156] D. J. Hollenbach, M. W. Werner and E. E. Salpeter, *Molecular Hydrogen in H I Regions*, *The Astrophysical Journal* **163** (Jan., 1971) 165.
- [157] M. Jura, *Formation and destruction rates of interstellar H₂*, *The Astrophysical Journal* **191** (July, 1974) 375–379.
- [158] S. Cazaux and A. G. G. M. Tielens, *Molecular Hydrogen Formation in the Interstellar Medium*, *The Astrophysical Journal* **575** (Aug., 2002) L29–L32, [[astro-ph/0207035](#)].
- [159] J. Le Bourlot, G. Pineau des Forêts and D. R. Flower, *The cooling of astrophysical media by H₂*, *Monthly Notices of the Royal Astronomical Society* **305** (May, 1999) 802–810.
- [160] M. Galametz, S. C. Madden, F. Galliano, S. Hony, G. J. Bendo and M. Sauvage, *Probing the dust properties of galaxies up to submillimetre wavelengths. II. Dust-to-gas mass ratio trends with metallicity and the submm excess in dwarf galaxies*, *Astronomy and Astrophysics* **532** (Aug., 2011) A56, [[1104.0827](#)].
- [161] R. Herrera-Camus, D. B. Fisher, A. D. Bolatto, A. K. Leroy, F. Walter, K. D. Gordon et al., *Dust-to-gas Ratio in the Extremely Metal-poor Galaxy I Zw 18*, *The Astrophysical Journal* **752** (June, 2012) 112, [[1204.4745](#)].
- [162] D. B. Fisher, A. D. Bolatto, R. Herrera-Camus, B. T. Draine, J. Donaldson, F. Walter et al., *The rarity of dust in metal-poor galaxies*, *Nature* **505** (Jan., 2014) 186–189.
- [163] T. A. Bell, E. Roueff, S. Viti and D. A. Williams, *Molecular line intensities as measures of cloud masses - I. Sensitivity of CO emissions to physical parameter variations*, *Monthly Notices of the Royal Astronomical Society* **371** (Oct., 2006) 1865–1872, [[astro-ph/0607428](#)].
- [164] S. Perlmutter, *Studying Dark Energy with Supernovae: Now, Soon, and the Not-Too-Distant Future*, *Physica Scripta Volume T* **117** (Jan., 2005) 17–28.
- [165] K. Krisciunas, P. M. Garnavich and e. a. Challis, P., *Hubble Space Telescope Observations of Nine High-Redshift ESSENCE Supernovae1,*, *The Astronomical Journal* **130** (Dec., 2005) 2453–2472, [[astro-ph/0508681](#)].
- [166] K. Nagamine and A. Loeb, *Future evolution of the intergalactic medium in a universe dominated by a cosmological constant*, *New Astronomy* **9** (Oct., 2004) 573–583, [[astro-ph/0310505](#)].
- [167] M. T. Busha, A. E. Evrard and F. C. Adams, *The Asymptotic Form of Cosmic Structure: Small-Scale Power and Accretion History*, *The Astrophysical Journal* **665** (Aug., 2007) 1–13, [[astro-ph/0611930](#)].
- [168] R. Dünner, P. A. Araya, A. Meza and A. Reisenegger, *The limits of bound structures in the accelerating Universe*, *Monthly Notices of the Royal Astronomical Society* **366** (Mar., 2006) 803–811, [[astro-ph/0603709](#)].
- [169] A. Loeb, *Long-term future of extragalactic astronomy*, *Physical Review D* **65** (Feb., 2002) 047301, [[astro-ph/0107568](#)].
- [170] A. Vilenkin, *Predictions from Quantum Cosmology*, *Physical Review Letters* **74** (Feb., 1995) 846–849, [[gr-qc/9406010](#)].
- [171] J. D. Barrow and F. J. Tipler, *The anthropic cosmological principle*. 1986.

- [172] G. Efstathiou, *An anthropic argument for a cosmological constant*, *Monthly Notices of the Royal Astronomical Society* **274** (June, 1995) L73–L76.
- [173] H. Martel, P. R. Shapiro and S. Weinberg, *Likely Values of the Cosmological Constant*, *The Astrophysical Journal* **492** (Jan., 1998) 29–40, [[astro-ph/9701099](#)].
- [174] S. Weinberg, *A priori probability distribution of the cosmological constant*, *Physical Review D* **61** (May, 2000) 103505, [[astro-ph/0002387](#)].
- [175] J. Garriga and A. Vilenkin, *Testable anthropic predictions for dark energy*, *Physical Review D* **67** (Feb., 2003) 043503, [[astro-ph/0210358](#)].
- [176] R. Bousso and J. Polchinski, *Quantization of four-form fluxes and dynamical neutralization of the cosmological constant*, *Journal of High Energy Physics* **6** (June, 2000) 006, [[hep-th/0004134](#)].
- [177] S. B. Giddings, S. Kachru and J. Polchinski, *Hierarchies from fluxes in string compactifications*, *Physical Review D* **66** (Nov., 2002) 106006, [[hep-th/0105097](#)].
- [178] A. Maloney, E. Silverstein and A. Strominger, *de Sitter Space in Non-Critical String Theory*, *NASA STI/Recon Technical Report N* **3** (June, 2002) , [[hep-th/0205316](#)].
- [179] S. Kachru, R. Kallosh, A. Linde and S. P. Trivedi, *de Sitter vacua in string theory*, *Physical Review D* **68** (Aug., 2003) 046005, [[hep-th/0301240](#)].
- [180] S. K. Ashok and M. R. Douglas, *Counting flux vacua*, *Journal of High Energy Physics* **1** (Jan., 2004) 060, [[hep-th/0307049](#)].
- [181] L. Susskind, *The Anthropic Landscape of String Theory*, in *The Davis Meeting On Cosmic Inflation*, p. 26, Mar., 2003. [[hep-th/0302219](#)].
- [182] S. Weinberg, *Living in the Multiverse*, *ArXiv High Energy Physics - Theory e-prints* (Nov., 2005) , [[hep-th/0511037](#)].
- [183] J. Polchinski, *The Cosmological Constant and the String Landscape*, *ArXiv High Energy Physics - Theory e-prints* (Mar., 2006) , [[hep-th/0603249](#)].
- [184] B. Moore, J. Diemand, P. Madau, M. Zemp and J. Stadel, *Globular clusters, satellite galaxies and stellar haloes from early dark matter peaks*, *Monthly Notices of the Royal Astronomical Society* **368** (May, 2006) 563–570, [[astro-ph/0510370](#)].
- [185] G. Meylan and D. C. Heggie, *Internal dynamics of globular clusters*, *Astronomy and Astrophysics* **8** (1997) 1–143, [[astro-ph/9610076](#)].
- [186] S. Mao and B. Paczynski, *Gravitational microlensing by double stars and planetary systems*, *The Astrophysical Journal* **374** (June, 1991) L37–L40.
- [187] B.-G. Park, Y.-B. Jeon, C.-U. Lee and C. Han, *Microlensing Sensitivity to Earth-Mass Planets in the Habitable Zone*, *The Astrophysical Journal* **643** (June, 2006) 1233–1238, [[astro-ph/0602006](#)].
- [188] M. Albrow, J.-P. Beaulieu, P. Birch and e. a. Caldwell, J. A. R., *The 1995 Pilot Campaign of PLANET: Searching for Microlensing Anomalies through Precise, Rapid, Round-the-Clock Monitoring*, *The Astrophysical Journal* **509** (Dec., 1998) 687–702, [[astro-ph/9807299](#)].
- [189] J. Yoo, D. L. DePoy, A. Gal-Yam and e. a. Gaudi, B. S., *Constraints on Planetary Companions in the Magnification $A=256$ Microlensing Event OGLE-2003-BLG-423*, *The Astrophysical Journal* **616** (Dec., 2004) 1204–1214, [[astro-ph/0403459](#)].
- [190] I. A. Bond, N. J. Rattenbury and e. a. Skuljan, J., *Study by MOA of extrasolar planets in gravitational microlensing events of high magnification*, *Monthly Notices of the Royal Astronomical Society* **333** (June, 2002) 71–83, [[astro-ph/0102184](#)].
- [191] A. Udalski, *The Optical Gravitational Lensing Experiment. Real Time Data Analysis Systems in the OGLE-III Survey*, *Acta Astronomica* **53** (Dec., 2003) 291–305, [[astro-ph/0401123](#)].

- [192] J.-P. Beaulieu, D. P. Bennett and e. a. Fouqué, P., *Discovery of a cool planet of 5.5 Earth masses through gravitational microlensing*, *Nature* **439** (Jan., 2006) 437–440, [[astro-ph/0601563](#)].
- [193] A. Gould, A. Udalski, D. An and e. a. Bennett, D. P., *Microlens OGLE-2005-BLG-169 Implies That Cool Neptune-like Planets Are Common*, *The Astrophysical Journal* **644** (June, 2006) L37–L40, [[astro-ph/0603276](#)].
- [194] B. S. Gaudi and A. Gould, *Planet Parameters in Microlensing Events*, *The Astrophysical Journal* **486** (Sept., 1997) 85–99, [[astro-ph/9610123](#)].
- [195] I. A. Bond, F. Abe, R. J. Dodd and e. a. Hearnshaw, J. B., *Improving the prospects for detecting extrasolar planets in gravitational microlensing events in 2002*, *Monthly Notices of the Royal Astronomical Society* **331** (Mar., 2002) L19–L23, [[astro-ph/0111041](#)].
- [196] G. Covone, R. de Ritis, M. Dominik and A. A. Marino, *Detecting planets around stars in nearby galaxies*, *Astronomy and Astrophysics* **357** (May, 2000) 816–822, [[astro-ph/9903285](#)].
- [197] E. A. Baltz and P. Gondolo, *Binary Events and Extragalactic Planets in Pixel Microlensing*, *The Astrophysical Journal* **559** (Sept., 2001) 41–52, [[astro-ph/9909509](#)].
- [198] S.-J. Chung, D. Kim, M. J. Darnley, J. P. Duke, A. Gould, C. Han et al., *The Possibility of Detecting Planets in the Andromeda Galaxy*, *The Astrophysical Journal* **650** (Oct., 2006) 432–437, [[astro-ph/0509622](#)].
- [199] A. P. Huxor, N. R. Tanvir, M. J. Irwin, R. Ibata, J. L. Collett, A. M. N. Ferguson et al., *A new population of extended, luminous star clusters in the halo of M31*, *Monthly Notices of the Royal Astronomical Society* **360** (July, 2005) 1007–1012, [[astro-ph/0412223](#)].
- [200] H. L. Morrison, P. Harding, D. Hurley-Keller and G. Jacoby, *Andromeda VIII: A New Tidally Distorted Satellite of M31*, *The Astrophysical Journal* **596** (Oct., 2003) L183–L186, [[astro-ph/0309254](#)].
- [201] R. Di Stefano and R. A. Scalzo, *A New Channel for the Detection of Planetary Systems through Microlensing. I. Isolated Events due to Planet Lenses*, *The Astrophysical Journal* **512** (Feb., 1999) 564–578, [[astro-ph/9808075](#)].
- [202] K. C. Sahu, *Stars Within the Large Magellanic Cloud as Potential Lenses for Observed Microlensing Events*, *Nature* **370** (July, 1994) 275.
- [203] G. Gyuk, N. Dalal and K. Griest, *Self-lensing Models of the Large Magellanic Cloud*, *The Astrophysical Journal* **535** (May, 2000) 90–103, [[astro-ph/9907338](#)].
- [204] D. Charbonneau, T. M. Brown, A. Burrows and G. Laughlin, *When Extrasolar Planets Transit Their Parent Stars*, *Protostars and Planets V* (2007) 701–716, [[astro-ph/0603376](#)].
- [205] J. Pepper and B. S. Gaudi, *Searching for Transiting Planets in Stellar Systems*, *The Astrophysical Journal* **631** (Sept., 2005) 581–596, [[astro-ph/0504162](#)].
- [206] G. Mallén-Ornelas, S. Seager, H. K. C. Yee, D. Minniti, M. D. Gladders, G. M. Mallén-Fullerton et al., *The EXPLORE Project. I. A Deep Search for Transiting Extrasolar Planets*, *The Astrophysical Journal* **582** (Jan., 2003) 1123–1140, [[astro-ph/0203218](#)].
- [207] S. Urakawa, T. Yamada, Y. Suto, E. L. Turner, Y. Itoh, T. Mukai et al., *Extrasolar Transiting Planet Search with Subaru Suprime-Cam*, *ArXiv Astrophysics e-prints* (Mar., 2006), [[astro-ph/0603346](#)].
- [208] A. Udalski, B. Paczynski, K. Zebrun, M. Szymanski, M. Kubiak, I. Soszynski et al., *The Optical Gravitational Lensing Experiment. Search for Planetary and Low-Luminosity Object Transits in the Galactic Disk. Results of 2001 Campaign*, *Acta Astronomica* **52** (Mar., 2002) 1–37, [[astro-ph/0202320](#)].

- [209] M. Konacki, G. Torres, S. Jha and D. D. Sasselov, *An extrasolar planet that transits the disk of its parent star*, *Nature* **421** (Jan., 2003) 507–509.
- [210] F. Bouchy, F. Pont, N. C. Santos, C. Melo, M. Mayor, D. Queloz et al., *Two new “very hot Jupiters” among the OGLE transiting candidates*, *Astronomy and Astrophysics* **421** (July, 2004) L13–L16, [[astro-ph/0404264](#)].
- [211] R. L. Gilliland, T. M. Brown and e. a. Guhathakurta, P., *A Lack of Planets in 47 Tucanae from a Hubble Space Telescope Search*, *The Astrophysical Journal* **545** (Dec., 2000) L47–L51.
- [212] S. Sigurdsson, H. B. Richer, B. M. Hansen, I. H. Stairs and S. E. Thorsett, *A Young White Dwarf Companion to Pulsar B1620-26: Evidence for Early Planet Formation*, *Science* **301** (July, 2003) 193–196, [[astro-ph/0307339](#)].
- [213] M. Ricotti and N. Y. Gnedin, *Formation Histories of Dwarf Galaxies in the Local Group*, *The Astrophysical Journal* **629** (Aug., 2005) 259–267, [[astro-ph/0408563](#)].
- [214] M. Ricotti, *Did globular clusters reionize the Universe?*, *Monthly Notices of the Royal Astronomical Society* **336** (Oct., 2002) L33–L37, [[astro-ph/0208352](#)].
- [215] J. E. Rhoads, A. Dey, S. Malhotra, D. Stern, H. Spinrad, B. T. Jannuzi et al., *Spectroscopic Confirmation of Three Redshift $z \sim 5.7$ Ly α Emitters from the Large-Area Lyman Alpha Survey*, *The Astronomical Journal* **125** (Mar., 2003) 1006–1013, [[astro-ph/0209544](#)].
- [216] J.-P. Kneib, R. S. Ellis, M. R. Santos and J. Richard, *A Probable $z \sim 7$ Galaxy Strongly Lensed by the Rich Cluster A2218: Exploring the Dark Ages*, *The Astrophysical Journal* **607** (June, 2004) 697–703, [[astro-ph/0402319](#)].
- [217] D. P. Stark and R. S. Ellis, *Searching for the sources responsible for cosmic reionization: Probing the redshift range $7 < z < 10$ and beyond*, *New Astronomy* **50** (Mar., 2006) 46–52, [[astro-ph/0508123](#)].
- [218] J. E. Rhoads and S. Malhotra, *Ly α Emitters at Redshift $z = 5.7$* , *The Astrophysical Journal* **563** (Dec., 2001) L5–L9, [[astro-ph/0110280](#)].
- [219] M. R. Santos, R. S. Ellis, J.-P. Kneib, J. Richard and K. Kuijken, *The Abundance of Low-Luminosity Ly α Emitters at High Redshift*, *The Astrophysical Journal* **606** (May, 2004) 683–701, [[astro-ph/0310478](#)].
- [220] R. J. Bouwens, G. D. Illingworth, P. A. Oesch, J. Caruana, B. Holwerda, R. Smit et al., *Reionization After Planck: The Derived Growth of the Cosmic Ionizing Emissivity Now Matches the Growth of the Galaxy UV Luminosity Density*, *The Astrophysical Journal* **811** (Oct., 2015) 140, [[1503.08228](#)].
- [221] R. J. Bouwens, G. D. Illingworth and e. a. Oesch, P. A., *UV Luminosity Functions at Redshifts $z=4$ to $z=10$: 10,000 Galaxies from HST Legacy Fields*, *The Astrophysical Journal* **803** (Apr., 2015) 34, [[1403.4295](#)].
- [222] A. E. Dolphin, D. R. Weisz, E. D. Skillman and J. A. Holtzman, *Star Formation Histories of Local Group Dwarf Galaxies*, *ArXiv Astrophysics e-prints* (June, 2005) , [[astro-ph/0506430](#)].
- [223] R. F. G. Wyse and G. Gilmore, *Stellar populations with ELTs*, in *The Scientific Requirements for Extremely Large Telescopes* (P. Whitelock, M. Dennefeld and B. Leibundgut, eds.), vol. 232 of *IAU Symposium*, pp. 140–148, 2006. [astro-ph/0604130](#). DOI.
- [224] M. Dietrich, F. Hamann, I. Appenzeller and M. Vestergaard, *Fe II/Mg II Emission-Line Ratio in High-Redshift Quasars*, *The Astrophysical Journal* **596** (Oct., 2003) 817–829, [[astro-ph/0306584](#)].
- [225] M. Fukugita, C. J. Hogan and P. J. E. Peebles, *The Cosmic Baryon Budget*, *The Astrophysical Journal* **503** (Aug., 1998) 518–530, [[astro-ph/9712020](#)].

- [226] R. Davé, R. Cen, J. P. Ostriker, G. L. Bryan, L. Hernquist, N. Katz et al., *Baryons in the Warm-Hot Intergalactic Medium*, *The Astrophysical Journal* **552** (May, 2001) 473–483, [[astro-ph/0007217](#)].
- [227] R. Cen and J. P. Ostriker, *Where Are the Baryons?*, *The Astrophysical Journal* **514** (Mar., 1999) 1–6, [[astro-ph/9806281](#)].
- [228] D. A. Fischer and J. Valenti, *The Planet-Metallicity Correlation*, *The Astrophysical Journal* **622** (Apr., 2005) 1102–1117.
- [229] G. Laughlin, P. Bodenheimer and F. C. Adams, *The End of the Main Sequence*, *The Astrophysical Journal* **482** (June, 1997) 420–432.
- [230] A. J. Rushby, M. W. Claire, H. Osborn and A. J. Watson, *Habitable Zone Lifetimes of Exoplanets around Main Sequence Stars*, *Astrobiology* **13** (Sept., 2013) 833–849.
- [231] S. J. Mojzsis, G. Arrhenius, K. D. McKeegan, T. M. Harrison, A. P. Nutman and C. R. L. Friend, *Evidence for life on Earth before 3,800 million years ago*, *Nature* **384** (Nov., 1996) 55–59.
- [232] J. W. Valley, W. H. Peck, E. M. King and S. A. Wilde, *A cool early Earth*, *Geology* **30** (Apr., 2002) 351.
- [233] G. Chabrier, *Galactic Stellar and Substellar Initial Mass Function*, *Publications of the Astronomical Society of Australia* **115** (July, 2003) 763–795, [[astro-ph/0304382](#)].
- [234] C. Conroy, A. A. Dutton, G. J. Graves, J. T. Mendel and P. G. van Dokkum, *Dynamical versus Stellar Masses in Compact Early-type Galaxies: Further Evidence for Systematic Variation in the Stellar Initial Mass Function*, *The Astrophysical Journal Letters* **776** (Oct., 2013) L26, [[1306.2316](#)].
- [235] M. Salaris and S. Cassisi, *Evolution of Stars and Stellar Populations*. 2006.
- [236] P. Madau and M. Dickinson, *Cosmic Star-Formation History*, *Annual Reviews of Astronomy and Astrophysics* **52** (Aug., 2014) 415–486, [[1403.0007](#)].
- [237] L. Barnes, M. J. Francis, G. F. Lewis and E. V. Linder, *The Influence of Evolving Dark Energy on Cosmology*, *Publications of the Astronomical Society of Australia* **22** (2005) 315–325, [[astro-ph/0510791](#)].
- [238] W. A. Traub, *Steps towards eta-Earth, from Kepler data*, *International Journal of Astrobiology* **14** (July, 2015) 359–363.
- [239] A. Silburt, E. Gaidos and Y. Wu, *A Statistical Reconstruction of the Planet Population around Kepler Solar-type Stars*, *The Astrophysical Journal* **799** (Feb., 2015) 180, [[1406.6048](#)].
- [240] E. A. Petigura, A. W. Howard and G. W. Marcy, *Prevalence of Earth-size planets orbiting Sun-like stars*, *Proceedings of the National Academy of Science* **110** (Nov., 2013) 19273–19278, [[1311.6806](#)].
- [241] G. W. Marcy, L. M. Weiss, E. A. Petigura, H. Isaacson, A. W. Howard and L. A. Buchhave, *Occurrence and core-envelope structure of 1-4 Earth-size planets around Sun-like stars*, *Proceedings of the National Academy of Science* **111** (Sept., 2014) 12655–12660, [[1404.2960](#)].
- [242] C. D. Dressing and D. Charbonneau, *The Occurrence of Potentially Habitable Planets Orbiting M Dwarfs Estimated from the Full Kepler Dataset and an Empirical Measurement of the Detection Sensitivity*, *The Astrophysical Journal* **807** (July, 2015) 45, [[1501.01623](#)].
- [243] S. Seager, W. Bains and R. Hu, *A Biomass-based Model to Estimate the Plausibility of Exoplanet Biosignature Gases*, *The Astrophysical Journal* **775** (Oct., 2013) 104, [[1309.6014](#)].
- [244] A. Loeb and D. Maoz, *Detecting biomarkers in habitable-zone earths transiting white dwarfs*, *Monthly Notices of the Royal Astronomical Society* **432** (May, 2013) 11–15, [[1301.4994](#)].

- [245] F. Rodler and M. López-Morales, *Feasibility Studies for the Detection of O₂ in an Earth-like Exoplanet*, *The Astrophysical Journal* **781** (Jan., 2014) 54, [[1312.1585](#)].
- [246] H. W. Lin and A. Loeb, *Statistical Signatures of Panspermia in Exoplanet Surveys*, *The Astrophysical Journal Letters* **810** (Sept., 2015) L3, [[1507.05614](#)].
- [247] R. K. Kopparapu, R. Ramirez, J. F. Kasting, V. Eymet, T. D. Robinson, S. Mahadevan et al., *Habitable Zones around Main-sequence Stars: New Estimates*, *The Astrophysical Journal* **765** (Mar., 2013) 131, [[1301.6674](#)].
- [248] S. N. Raymond, J. Scalo and V. S. Meadows, *A Decreased Probability of Habitable Planet Formation around Low-Mass Stars*, *The Astrophysical Journal* **669** (Nov., 2007) 606–614, [[0707.1711](#)].
- [249] J. E. Owen and S. Mohanty, *Habitability of terrestrial-mass planets in the HZ of M Dwarfs - I. H/He-dominated atmospheres*, *Monthly Notices of the Royal Astronomical Society* **459** (July, 2016) 4088–4108, [[1601.05143](#)].
- [250] B. Carter, *The Anthropic Principle and its Implications for Biological Evolution*, *Philosophical Transactions of the Royal Society of London Series A* **310** (Dec., 1983) 347–363.
- [251] J. Laskar, F. Joutel and P. Robutel, *Stabilization of the earth’s obliquity by the moon*, *Nature* **361** (Feb., 1993) 615–617.
- [252] R. G. Martin and M. Livio, *On the formation and evolution of asteroid belts and their potential significance for life*, *Monthly Notices of the Royal Astronomical Society* **428** (Jan., 2013) L11–L15, [[1211.0023](#)].
- [253] N. Haghighipour and L. Kaltenegger, *Calculating the Habitable Zone of Binary Star Systems. II. P-type Binaries*, *The Astrophysical Journal* **777** (Nov., 2013) 166, [[1306.2890](#)].
- [254] C. H. Lineweaver, Y. Fenner and B. K. Gibson, *The Galactic Habitable Zone and the Age Distribution of Complex Life in the Milky Way*, *Science* **303** (Jan., 2004) 59–62, [[astro-ph/0401024](#)].
- [255] T. Piran and R. Jimenez, *Possible Role of Gamma Ray Bursts on Life Extinction in the Universe*, *Physical Review Letters* **113** (Dec., 2014) 231102, [[1409.2506](#)].

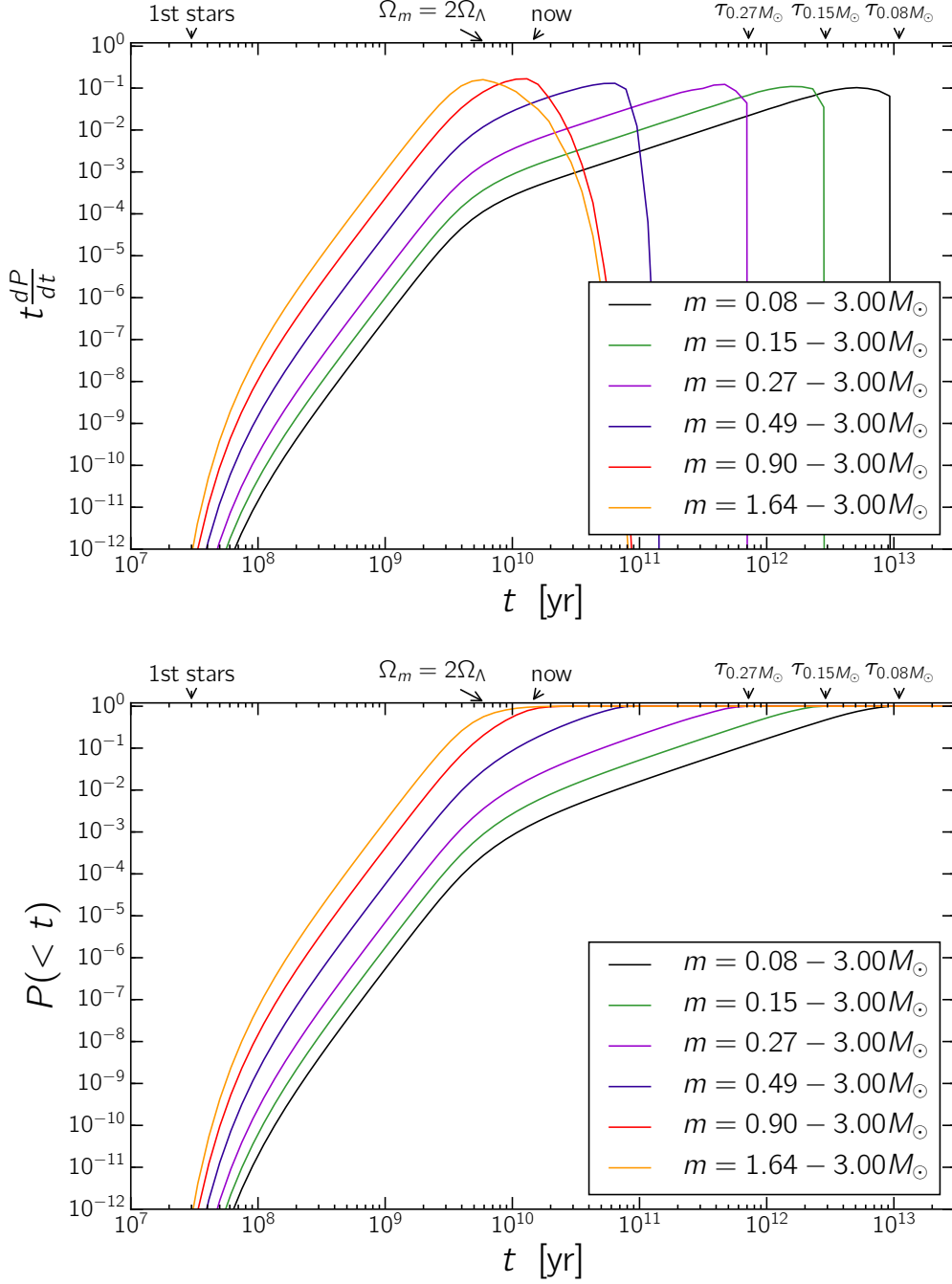


Figure 11. Probability distribution for the emergence of life within a fixed comoving volume of the Universe as a function of cosmic time. We show the probability per log time, $t dP/dt$ (top panel) as well as the cumulative probability up to a time t , $P(< t)$ (bottom panel), for different choices of the minimum stellar mass, equally spaced in log m between $0.08 M_\odot$ and $3 M_\odot$. The contribution of stars above $3 M_\odot$ to $dP(t)/dt$ is ignored due to their short lifetimes and low abundances. The labels on the top axis indicate the formation time of the first stars, the time when the cosmic expansion started accelerating (i.e., when the density parameter of matter, Ω_m , was twice that of the vacuum, Ω_Λ), the present time (now) and the lifetimes of stars with masses of $0.08 M_\odot$, $0.15 M_\odot$ and $0.27 M_\odot$.